FLUORESCEIN, ACRYLODAN AND PYRENE CONJUGATES OF HORSE PLASMA GELSOLIN: RESPONSES TO CALCIUM, ACTIN AND TROPOMYOSIN

By

EDWARD KURT KOEPF

B.Sc., The University of Victoria, 1990

A THESIS SUBMITTED IN PARTIAL FULFILLMENT OF
THE REQUIREMENTS FOR THE DEGREE OF
MASTER OF SCIENCE

in

THE FACULTY OF GRADUATE STUDIES
(Department of Chemistry)

We accept this thesis as conforming
to the required standard

THE UNIVERSITY OF BRITISH COLUMBIA
August 1992

In presenting this thesis in partial fulfilment of the requirements for an advanced degree at the University of British Columbia, I agree that the Library shall make it freely available for reference and study. I further agree that permission for extensive copying of this thesis for scholarly purposes may be granted by the head of my department or by his or her representatives. It is understood that copying or publication of this thesis for financial gain shall not be allowed without my written permission.

Department of Chemistry

The University of British Columbia
Vancouver, Canada

Date Aug. 31, 1992

DE-6 (2/88)

Abstract

Gelsolin, a protein involved in the regulation of actin filament length, was isolated from horse plasma and modified with the amine-selective reagent fluorescein-5-isothiocyanate (FITC). The extent of FITC incorporation per gelsolin molecule was 4.8 ± 0.6, based upon 4 labelling trials. FITC-gelsolin analysed by SDS-PAGE revealed a single fluorescent band under UV light prior to staining, and then a single Coomassie Blue stained band. Viscosity studies showed that gelsolin's F-actin severing activity was not impaired upon reaction with FITC, but incorporation of the fluorophores did increase the the temperature at which the onset of irreversible precipitation occurred.

Under physiological ionic conditions, fluorescence studies failed to detect a Ca^{+2} effect on FITC-gelsolin's spectroscopic characteristics, but in low ionic strength solutions, Ca^{+2} increased the fluorescence intensity by approximately 25%. A calcium effect was also evident in bimolecular fluorescence quenching studies with KI, which showed that Ca^{+2} rendered the fluorescence more susceptible to quenching. Subsequent protein denaturation with guanidine-HCl resulted in further exposure of the fluorescein chromophores to iodide in solvent.

An investigation of reactivity with the thiol selective reagents acrylodan (ACR) and pyrene iodoacetamide (PIA) revealed that native gelsolin exposes 1 to 2 cysteine groups for reaction. Under denaturing conditions, the extent

of reaction increased to approximately 3 with ACR and 4 with PIA. In comparison, the average number of thiol groups available for reaction with 5,5'-dithiobis(2-nitrobenzoic acid) was approximately 1, and 3 to 4 in native and denaturing conditions, respectively.

Actin-gelsolin complexation was revealed by fluorescence titrations and fluorescence polarization measurements. Addition of actin to FITC-labelled gelsolin increased the fluorescence intensity of the sample in a Ca^{+2} specific manner, while binding of actin to ACR-gelsolin resulted in a fluorescence decrease. Fluorescence polarization values increased on addition of actin to both FITC- and ACR-labelled gelsolin solutions only in the presence of Ca^{+2}, establishing the calcium requirement for actin binding.

Tropomyosin binding to gelsolin was evident from an increase in the fluorescence intensity of FITC-labelled gelsolin, and from retention of labelled gelsolins on a tropomyosin-agarose affinity column. Quantitative assessment of a direct titration of FITC-labelled gelsolin with tropomyosin yielded two independent tropomyosin binding sites on gelsolin, with a dissociation constant of approximately 0.6 μM. Both of these effects required the presence of micromolar Ca^{+2}. Photoactivation of solutions of benzophenone-4-isothiocyanate labelled gelsolin and tropomyosin resulted in the appearance of high molecular weight bands on SDS-PAGE, indicative of intermolecular crosslinking.

Table of Contents

CHAPTER 2 MATERIALS AND METHODS

CHAPTER 3 RESULTS AND DISCUSSION

List of Tables

List of Figures

Abbreviations

ACR	Acrylodan
ACRG	Acrylodan-labelled gelsolin
ADP	Adenosine 5'-diphosphate
ATP	Adenosine 5'-triphosphate
BITC	Benzophenone-4-isothiocyanate
Buffer A	2 mM Tris-HCl, 1 mM DTT, 0.2 mM ATP, 0.2 mM $CaCl_2$, pH 7.6
CD	Circular dichroism
C-TM	Cardiac muscle tropomyosin
Cys	Cysteine amino acid
DBP	Vitamin-D-binding protein
DEAE	Diethylaminoethyl
DMF	N,N-dimethylformamide
DMSO	Dimethyl sulfoxide
DTNB	5,5'-dithiobis(2-nitrobenzoic acid)
DTT	D,L-dithiothreitol
EDTA	Ethylenediaminetetraacetic acid
EGTA	1,2-Di(2-aminoethoxy)ethane-N,N,N',N'-tetraacetic acid
F-actin	Polymerised filamentous actin
FITC	Fluorescein-5-isothiocyanate
G-actin	Monomeric globular actin
Hepes	N-2-Hydroxyethylpiperazine-N'-2-ethanesulfonic acid
Mops	3-(N-Morpholino)propanesulfonic acid
L	Left circularly polarized light
Lys	Lysine amino acid

PIA	N-(1-pyrene)iodoacetamide
PMSF	Phenylmethylsulfonyl fluoride
PAGE	Polyacrylamide gel electrophoresis
PIP	Phosphatidylinositol 4-phosphate
PIP_2	Phosphatidylinositol 4,5-bisphosphate
R	Right circularly polarized light
SDS	Sodium dodecyl sulfate
S-TM	Skeletal tropomyosin
Tris-HCl	Tris(hydroxymethyl)aminomethane hydrochloride

Acknowledgements

I would like to thank Dr. Les Burtnick for his guidance and support during the course of this project and for helpful discussions on the content of the thesis. Special thanks to my parents for all their support.

Chapter 1

INTRODUCTION

I. Proteins

1.1 Actin

The discovery of actin and its introduction to the scientific literature has been accredited to Straub, who in 1942, identified this protein as a major muscle tissue constituent.[1,2] In the first thirty years after its discovery the majority of actin research focused on its involvement in contractile movement, a process whereby chemical energy stored in muscle cells is converted to mechanical energy. The field of non-muscle actin research did not gain prominence until the mid-1960s when, for the first time, highly pure actin was isolated from slime molds. Following this discovery, it quickly became evident that all eukaryotic cells contain actin, comprising as much as 20% of the total protein content in certain cells.[3]

Actin is not only a very abundant protein, it is also one of the most evolutionarily conserved proteins studied to date. This high degree of conservation is thought to be a reflection of a strong selective pressure that is exerted upon actin, one which is responsible for preserving actin's tertiary structure. Essential interaction sites which are required for the many

regulatory factors that bind to actin are maintained by keeping this structure intact.[4] Actin's involvement in such diverse cellular functions as muscle contraction, cytoplasmic streaming, hearing, transport, nutrient absorption, secretion, phagocytosis, and cytokinesis commands the participation of a number of regulatory components known collectively as actin binding proteins.[5]

The biological activity of actin in non-muscle cells is linked to this protein's ability of self-association from monomeric G-actin into noncovalent, helical filamentous F-actin.[6] The G-actin monomer is relatively globular with a molecular mass of 42 000 daltons. It tightly binds one molecule of ATP as well as one divalent metal ion, either Mg^{+2} or Ca^{+2}. Actin also exposes a series of lower affinity metal binding sites which are capable of binding either mono- or divalent cations.[5]

F-actin filaments are linear polymers which consist of two staggered, parallel rows of actins twisted into a right-handed helix that may attain lengths of several microns.[5,7] Electron microscopic studies show that there are 13 subunits in the two strands between each crossover point, and 13 subunits in a single strand per 72 nm helical pitch (figure 1).[3,8] The distance between consecutive crossover points is estimated at approximately 36 nm along the helical axis. Although F-actin appears rod-like, the filaments do exhibit some torsional flexibility with fluctuations of 5-10 degrees.

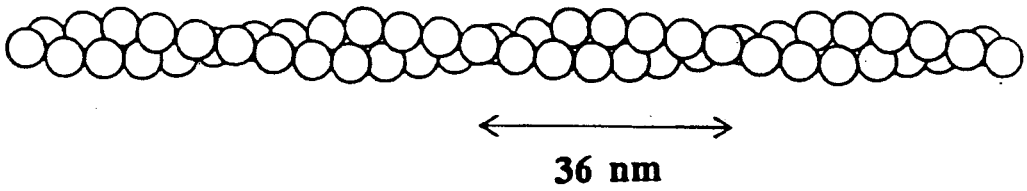

Figure 1 : Schematic diagram of the helical array of the two staggered, parallel rows of actin monomers in F-actin.

Incorporation of G-actin into the F-actin filament may occur at either of the two ends of the growing polymer. Kinetic studies have demonstrated that assembly and disassembly rates at the two polymer ends are not equal.[4] The end which exhibits preferred assembly is referred to as the barbed (B), or the (+) end, while preferential disassembly occurs at the pointed (P), or (-) end. A result that arises from these differential rates is that actin filaments attain a polarity. Electron micrographs of filaments decorated with the myosin subfragment 1, a proteolytic fragment from the other major component of the contractile system, reveal a distinctive arrowhead pattern (figure 2).[8] Analogies of such arrowhead patterns with flights on an arrow are the basis of the pointed and barbed nomenclature.

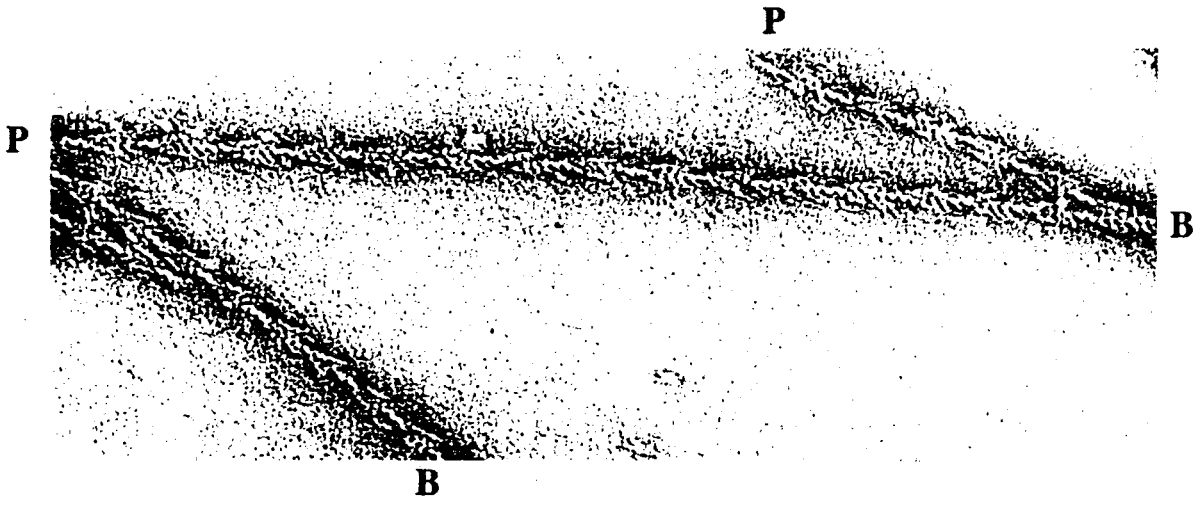

Figure 2 : Electron micrograph of F-actin filaments decorated with myosin subfragment 1. P and B represent the pointed and barbed ends, respectively.

1.2 Polymerization of Actin

Many of the mechanistic details of actin polymerization have been thoroughly investigated, although not all aspects are elucidated to date. The polymerization reaction is spontaneous, fully reversible, and in the absence of other proteins the polymerization extent is determined by temperature, pH, and ionic strength.[5] The subunits within the polymer are held together by predominately hydrophobic and some electrostatic forces, with perhaps some hydrogen bonding contributions.[7] Experimentally, actin polymerization may be induced in a number of ways which usually involve low concentrations of

$MgCl_2$, high concentrations of KCl, or a mixture of both. Our current understanding of the polymerization process takes into account at least four, well defined steps: monomer activation, nucleation, elongation, and filament annealing.[9]

The process of monomer activation is associated with a rapid change in G-actin conformation prior to nucleus formation or monomer incorporation. In the presence of either Ca^{+2} or Mg^{+2} and ATP, a cation-ATP-actin complex with a specific conformation forms. The recent three dimensional structure of the Ca-ATP-actin complex at 2.8 Å resolution shows the bound nucleotide, as well as the interactions that occur between the divalent cation and the β and γ phosphates of ATP.[10] The ATP-actin complex constitutes the high affinity metal binding site, characterised by an affinity constant which has been estimated in the range of 10^9 M^{-1} for the Mg^{+2} ion.[6] Further ligation of the Ca-ATP-actin or the Mg-ATP-actin complex with either mono- or divalent cations at the low affinity sites induces a conformational change which activates the monomer for polymerisation.

Following monomer activation is nucleation, a stage where the growth of a protofilament into filaments becomes more probable than its dissociation back to monomers.[9] This step is slow, rate-limiting, and readily observable during the time course of spontaneous polymerization (figure 3).[3] Such a plot is sigmoidal, showing an initial lag phase that has been attributed to the

nucleation process. Based on kinetic analysis, the general consensus is that the nucleus is a trimer, one derived from a dimer and a monomer.[6,9]

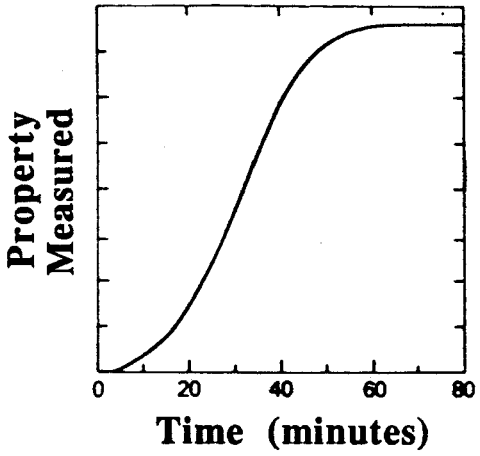

Figure 3 : Time course of salt induced actin polymerization. Nucleation accounts for the initial slow phase and filament elongation is attributed to the rapid phase.

Filament elongation results from the association of actin monomers with stable nuclei. Polymer growth is bidirectional, with preferred elongation taking place at the barbed end. Associated with, but not directly coupled to elongation is the hydrolysis of monomer bound ATP. An observable time delay between monomer addition and nucleotide hydrolysis indicates that the free energy liberated from the hydrolysis of ATP is not required for monomer incorporation.[9] The ATP hydrolysis in question occurs in two distinct steps; the actual chemical cleavage of the nucleotide occurs first, followed by the slow release of inorganic phosphate (P_i). Such a hydrolytic

mechanism serves to create F-actin filaments that contain regions of ATP-actin, ADP-P_i-actin, and ADP-actin. The regions of fast polymer growth exhibit ATP-actin subunits, whereas depolymerizing regions contain ADP-actin subunits. Conversion of ATP- to ADP-actin within F-actin filaments helps to destabilise individual actin-actin interactions, a process in which the slow release of P_i from ADP-P_i-actin plays an important role.[6]

In the absence of actin binding proteins the fate of F-actin filaments is described by two mechanisms. One of these assumes internal breakage of individual filaments into smaller fragments, each capable of further polymerization. The other mechanism involves separate F-actin fragments annealing together to quickly form very long filaments. Although both are quite likely to occur, no direct evidence is available for either mechanism, mainly because of experimental shortcomings in quantifying filament lengths in solution.[9]

1.3 Actin Binding Proteins

Actin's involvement in many diverse cellular functions is attributable to the various three dimensional structures that F-actin filaments assume upon polymerization. The dynamic rearrangement of one structure to another influences cell form and function, and is therefore highly regulated.[5,11] A diverse group of proteins that exhibit pronounced influences on actin filament structure has been identified, and termed actin binding proteins (figure 4).[12]

Classifications made in accordance with their *in vitro* behaviour have yielded three general groups: monomer sequestering proteins, capping and severing proteins, and crosslinking proteins.[5,9,11]

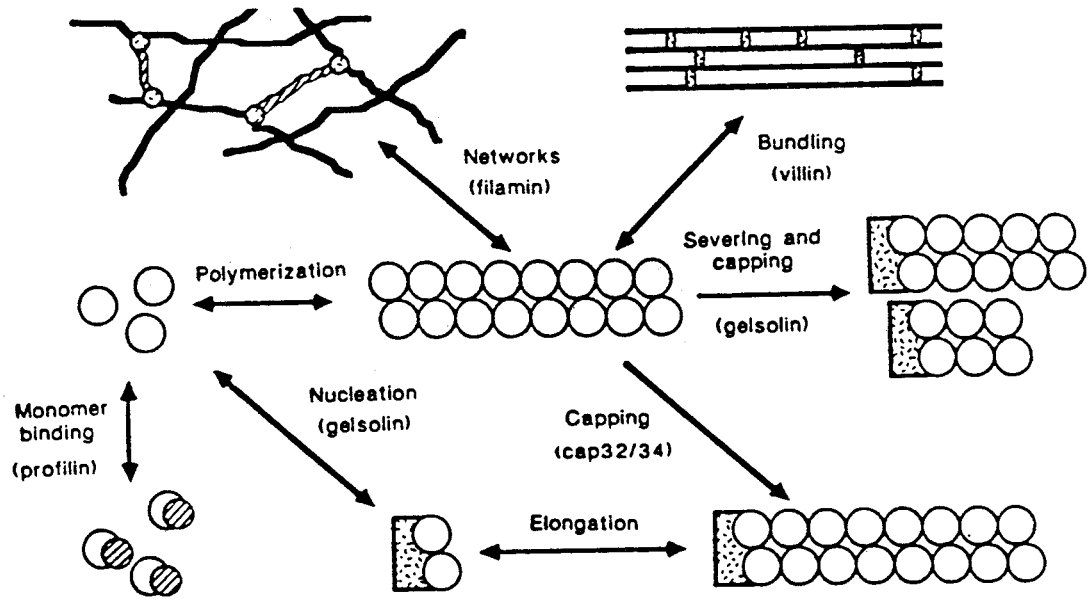

Figure 4 : Schematic illustration of actin binding proteins and their associations with G and F-actin. Representative proteins of each category are shown in parentheses.

The monomer sequesterers are a group of proteins that bind to G-actin to form a complex that does not polymerize readily. Prevention of spontaneous, unneeded polymerization ensures the availability of a pool of G-actin monomers that subsequently, when required, may be directed by intracellular signals to assemble into filaments.[7,8] These proteins have the ability to raise the G-actin concentration above the critical concentration, which by definition, is the minimal concentration of G-actin required to initiate polymerization.[4]

The capping or end-blocking proteins bind to F-actin filament ends influencing subunit interactions at those sites.[9] The majority of capping proteins identified to date bind at the barbed end of actin filaments. Severing proteins also bind to filaments, but they do so at internal regions of the polymer causing filament cleavage. This occurs by the disruption of the non-covalent actin-actin interactions. In addition to severing, many of these proteins also promote nucleation by generating an increased concentration of uncapped filament ends at which monomers can add.[4] The combined action of severing and nucleation minimises the presence of long filaments, and results in the formation of many short ones.

The third major group of actin binding proteins are the crosslinkers. These crosslink actin filaments, creating a multitude of three dimensional structures that range from highly organised bundles to isotropic gels.[4] Bundles or gels may associate further to form even higher levels of structure,

or they may interact with membranes or organelles.

1.4 Tropomyosin and the Troponin Complex

Intimately associated with the muscle contractile system is tropomyosin, a protein found in all muscle tissues as well as in a number of non-muscle cells. This protein binds along the sides of F-actin filaments, but displays no fragmentation or crosslinking abilities.[5] Skeletal muscle tropomyosin (S-TM) is a protein that consists of two highly α-helical polypeptide chains wound around each other to form a rope-like molecule which is commonly described as a coiled-coil structure.[13] Head to tail polymerization of the tropomyosin molecule yields long, unbroken strands that extend along both grooves of the actin filament (figure 5).[14] Each single tropomyosin spans seven actin subunits within a filament.

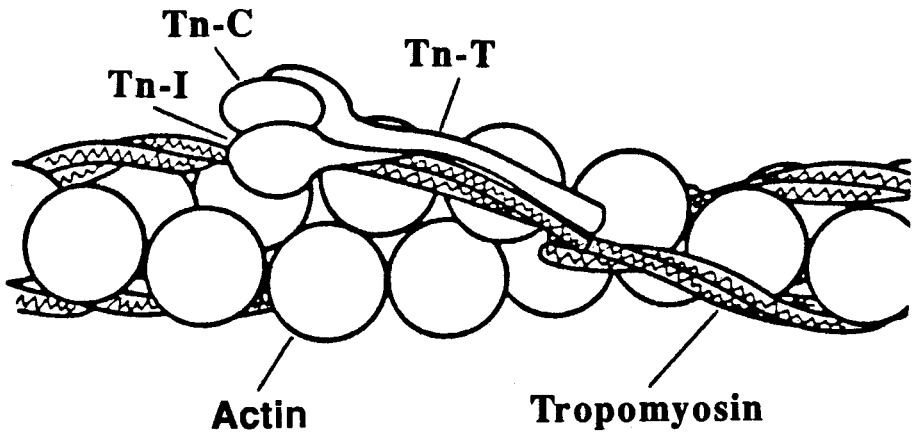

Figure 5 : Proposed model of the striated muscle thin filament showing the tropomyosin and troponin interactions with the actin filament.

The troponin complex is a group of three separate polypeptides that bind to S-TM. The constituents of this complex are the calcium-binding protein (troponin C), the tropomyosin-binding protein (troponin T), and the inhibitor protein (troponin I).[13] Specific interactions between S-TM, actin and the troponin complex constitute a switch which regulates muscle contraction. Saturation of troponin C with Ca^{+2} induces a conformational change within the troponin complex, which in turn, alters the tropomyosin position along the F-actin filament. It is thought that prior to the Ca^{+2} stimulus the tropomyosin molecule blocks the accessibility of myosin to F-actin, thereby preventing muscle contraction.

Tropomyosins isolated from non-muscle cells also exist as highly α-helical coil-coiled structures, but their sizes are smaller than their S-TM counterparts. Immunofluorescence studies with cultured non-muscle cells have shown that tropomyosin is localised with relatively static F-actin structures such as bundles or cables, but not with cellular regions exhibiting motility, places where actin filaments undergo dynamic changes.[14] Although non-muscle tropomyosins mirror many of the skeletal tropomyosin properties, their *in vivo* functions have yet to be defined.

1.5 Gelsolin

As a member of the capping and severing group of actin binding proteins, gelsolin's interactions with actin are multiple and complex.

Gelsolin has the capability of controlling *in vitro* linear actin assembly by severing actin filaments, by capping the barbed filament ends, and by nucleating actin filament assembly. This protein was first discovered in rabbit lung macrophages by Yin and Stossel in 1979, who derived the gelsolin name for its ability to convert actin gels to sols.[15,16] Actin gels are semi-rigid masses of crosslinked filaments, whereas sols are dispersions of filament fragments in solution. In the past decade gelsolin has been isolated from a wide variety of vertebrate species, and found to be synthesised by an assortment of cell types as both an intracellular and as a secreted isoform, best characterised from blood plasma.[17-22]

Cytoplasmic and plasma gelsolins are structurally and functionally quite similar. Genomic analysis revealed that the RNA messages for the two proteins are derived from the same gene through an elaborate pattern of RNA splicing, and alternative transcription initiation.[23,24] Both gene products consist of a single polypeptide chain with approximate molecular masses of 80 and 83 kDa respectively, for the cytoplasmic and plasma isoforms, but migrate with apparent molecular masses of 90 and 93 kDa on polyacrylamide gel electrophoresis in the presence of sodium dodecyl sulfate (SDS).[23,25] The molecular mass difference between these two proteins is attributable to an amino acid extension found at the N-terminal of the plasma variant; a sequence of amino acids which displays the typical features of a signal peptide.[23,26]

Complementary DNA sequence analysis of human and pig plasma gelsolins has revealed the occurrence of a strong tandem repeat in the amino acid sequence.[25] The two repeats, which are thought to be the result of an evolutionary gene duplication event, divide the gelsolin molecule into roughly equal amino and carboxy terminal domains. Further strong internal repeats of a shorter motif are also evident in the primary sequence. Six of these smaller repeats are found in gelsolin and referred to as S1-S6 (segments 1-6), based upon the nomenclature of Way and Weeds.[25] These smaller repeats have also been localised in villin, severin, and in fragmin, three other proteins capable of actin severing.

1.6 Gelsolin-Actin Interactions

Elucidating gelsolin's mode of action requires an investigation of gelsolin-actin interactions and the regulatory role that Ca^{+2} plays in those.[27] Segmental deletion mutagenesis and proteolytic cleavage studies have identified three actin interface regions on gelsolin, although in its native state gelsolin only binds two actin molecules.[28-30] Calcium ions bind to two distinct sites on gelsolin, and micromolar quantities of this cation are required for actin-gelsolin complexation. Calcium binding to gelsolin induces a conformational change which undoubtedly is an essential requirement for gelsolin to function.[31,32]

In the presence of micromolar calcium, gelsolin (G), binds two actin monomers (A), to form an A_2G complex. Chelation of the Ca^{+2} by the addition of EGTA dissociates one actin molecule, leaving an EGTA-resistant AG complex that retains one calcium ion.[33] This 1:1 actin-gelsolin complex is capable of nucleating actin monomer assembly and blocks filament ends with high affinity, but is incapable of severing F-actin.[33,34] Of the three effects that gelsolin has on actin, severing is the one that exhibits the most stringent calcium requirements.[35] This occurs in the micromolar Ca^{+2} concentration range, a range through which cells are able to exhibit control over free intracellular calcium levels. After severing, gelsolin remains tightly bound to the barbed end of the fragmented filament, forming a protective cap that does not dissociate even upon the removal of calcium ions.[36,38]

1.7 Gelsolin in the Cytoskeleton

Cytoplasmic gelsolin's *in vivo* function still remains somewhat unclear, although its role in controlling linear actin assembly in response to transient rises in cytosolic calcium is slowly being identified. Because gelsolin activity is dependent on Ca^{+2} concentrations, the process of actin reorganisation may ultimately be controlled by factors which regulate intracellular calcium levels. Additional regulatory control may be bestowed upon gelsolin by

polyphosphoinositides, phospholipids which are known to undergo rapid turnover during cell stimulation.[39,]

Uncapping gelsolin-blocked actin filaments, dissociation of the EGTA-resistant actin-gelsolin complex, and severing inhibition are observable when gelsolin binds either phosphatidylinositol 4-phosphate (PIP), or phosphatidyl-inositol 4,5-bisphosphate (PIP_2).[39,40] PIP_2 has also been noted for its abilities to dissociate a 1:1 actin complex formed with the monomer sequesterer profilin.[41] Based upon these observations a mechanism which may promote explosive actin filament growth has been proposed.[42,43] An initial Ca^{+2} concentration increase, and the hydrolysis of PIP_2 is thought to facilitate actin filament severing, which creates a large number of short, capped filaments. Subsequent rises in polyphosphoinositide levels release the sequestered actin that is bound to profilin, and uncaps the barbed end of actin filaments, which provides ready made actin nuclei for rapid polymerization.[42,43] Actin filaments with ends blocked by gelsolin are the key intermediates in this model for eliciting actin assembly at locations where cell surface receptors cause appropriate changes in polyphosphoinositide concentrations, conformations, or both.

1.8 Gelsolin in Plasma

The two plasma components that depolymerize filamentous actin are

plasma gelsolin and the vitamin-D-binding protein (DBP). The combined action of these two proteins, both of which are present in micromolar concentrations, forms an actin scavenging system.[44] The ionic conditions of plasma are such that any actin introduced into it, whether by physiological or pathological cell death, would be expected to polymerize into filaments.[45] Circulating filaments in plasma could potentially increase plasma viscosity, which would seriously impede blood flow through microcirculatory vessels.

The clearance of actin from plasma transpires in two steps. The first of these is rapid and attributable to direct filament severing by gelsolin. The second step, which is slower than severing, involves actin-DBP complexation.[44] DBP associates with monomeric actin to form a tight 1:1 stoichiometric complex, but does not interact with filaments.[46,47] Actin-DBP complexes are then rapidly cleared by the liver at a rate comparable to the clearance of actin from blood.[48] Since DBP has a higher affinity for actin than does gelsolin, the gelsolin present in plasma is expected to be free of actin. Preventing actin-gelsolin complexation in plasma by preferentially forming actin-DBP complexes conserves the filament severing activity of plasma gelsolin.[48]

II. Optical Techniques

2.1 Fluorescence Spectroscopy

Electronic absorption and emission spectra of molecules provide important information concerning the structure, energetics, and dynamics of electronically excited states. Because of the different time scales on which these two events occur, the molecular properties revealed by light emission are quite different than those obtained from light absorption.

Several factors inherent to fluorescence spectroscopy have contributed to its widespread applicability in life sciences. Perhaps the two most desired attributes of fluorescence are its sensitivity and selectivity. A high degree of sensitivity allows one to work at very low sample concentrations, while selective excitation of a desired chromophore permits one to probe specific molecular subunits. Fluorescence applications are routinely applied in studies of conformational heterogeneity, inter and intramolecular interactions, and in enzyme kinetics.[49]

When a molecule absorbs a photon of light, an electron is promoted from the highest occupied molecular orbital to one of the lowest energy, unoccupied molecular orbitals. Excitation from the electronic ground state to vibrationally excited levels of the first or higher electronic states occurs in approximately 10^{-15} seconds.

Since nuclear motions are on the order of 10^{-14} to 10^{-12} seconds, no significant nuclear displacements occur during the absorption process (Franck-Condon principle).[50] The events that return the excited metastable state back to thermal equilibrium are considerably slower, some lasting for seconds.

Deactivation of the excited state is achieved by a combination of radiative and non-radiative events. Unimolecular decomposition, isomerization, and ionization are a series of non-radiative photochemical events, while vibrational relaxation, internal conversion, intersystem crossing, and radiative emission are photophysical phenomena.[51] These various photophysical processes and their relations to excited states are illustrated by a Jablonski energy diagram (figure 6).[52] Light absorption by a molecule originating in S_o, the singlet ground state, produces an excited singlet state (S_1, S_2, etc.) in an upper vibrational level. Thermal relaxation to the lowest vibrational level of the electronically excited state is quickly achieved by collisions with solvent molecules. The excited state may further dissipate excitation energy by internal conversions from higher electronically excited levels to S_1.

Spin allowed radiative emission from S_1 to S_o occurs in approximately 10^{-8} seconds and is known as fluorescence. Alternatively, molecules in the S_1 state may intersystem cross to populate T_1, the lowest excited triplet state, an event that is classically forbidden.

Triplet excited states are very long lived (10^{-5} seconds to several seconds), which allows chemical and physical processes to compete effectively with phosphorescence, the emission of light from T_1 to S_o.

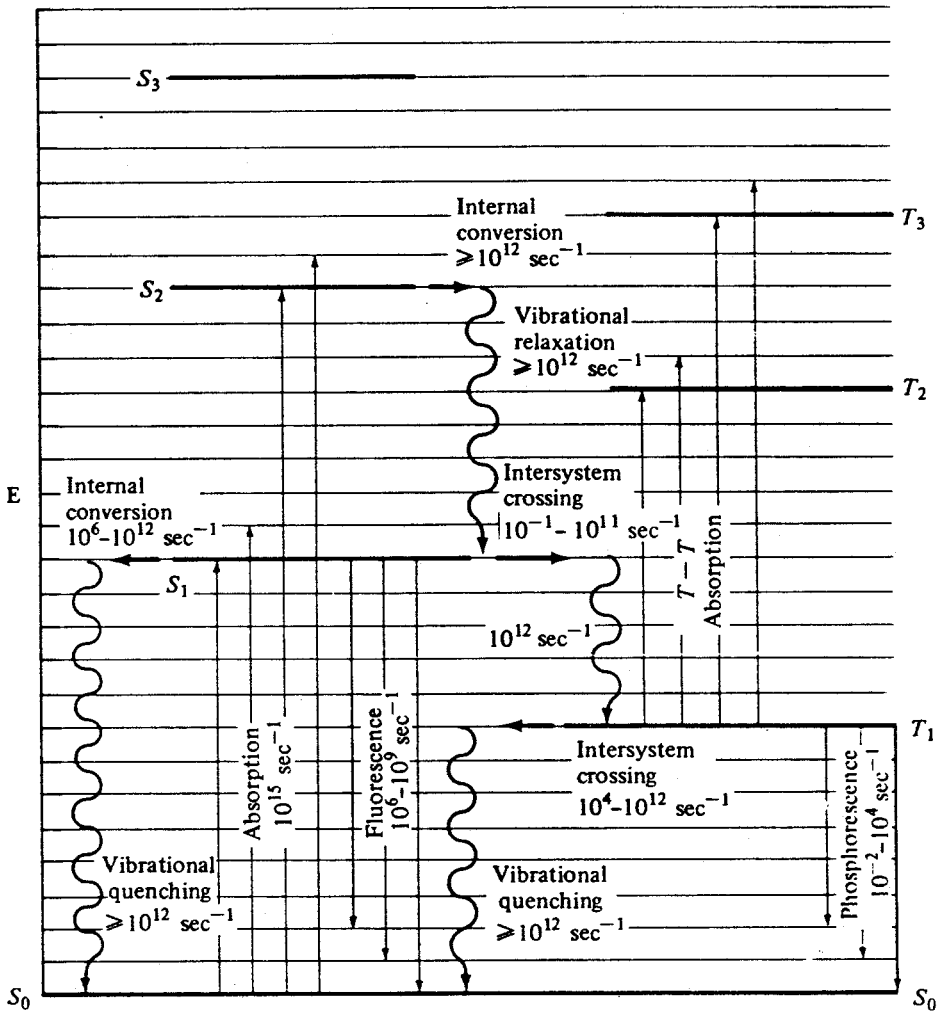

Figure 6 : Jablonski diagram. Lowest energy levels of a state are indicated by thick horizontal lines, while other horizontal lines represent associated vibrational levels. Radiative transitions are shown by vertically straight lines and non-radiative ones by wavy lines.

Not all excited molecules return to their ground state via fluorescence because of all the processes that compete to deactivate S_1. The fraction of excited molecules that do fluoresce is known as the fluorescence quantum yield (Φ_F), which is a physical constant of the excited molecular species at a given set of conditions. Stated in terms of rates that return S_1 to S_0, Φ_F is given by

$$\Phi_F = k_f / (k_f + \Sigma k_d)$$

where k_f is the rate constant for fluorescence and Σk_d is the sum of all other rate constants that deactivate S_1 by radiationless processes.

The intensity of fluorescence at a time t after the removal of the excitation source is given by the exponential relation

$$I(t) = I_o \exp(^{-}t/\tau_f)$$

where I_o is the initial intensity at time zero, and τ_f is the fluorescence lifetime. The reciprocal of ($k_f + \Sigma k_d$) yields the fluorescent lifetime, which gives an indication of how long a molecule spends in the excited state.

2.2 Solvent Effects

The fluorescence emission spectra of a number of fluorophores are sensitive to their environment. This phenomenon has resulted in numerous fluorescence applications dealing with fluorophores bound to proteins, membranes, nucleic acids, and to other complex macromolecular assemblies.

Solvent sensitivity has been extensively used to study protein binding sites, and to monitor macromolecular interactions.

The origin of the solvent effect comes from general physical interactions that occur between the fluorophore's dipole moment and the induced reactive fields from the surrounding solvent, and from specific chemical fluorophore-solvent interactions. A transition from S_0 to S_1 leaves the molecule in the initial Franck-Condon state which has S_0 geometry and solvation. Reorientation of the ground state solvent cage in response to a new electronic distribution creates an excited state different, and generally lower in energy than the Franck-Condon one. When fluorescence occurs from this lower energy state, it terminates in the ground electronic state of the solute molecule, but because of the rapidity of the transition the molecule is still associated with S_1 geometry and solvation (figure 7).[53] The energy difference between the absorption and the emission maxima, which is known as the Stokes shift, is a reflection of the energy loss induced by the solvent effect.

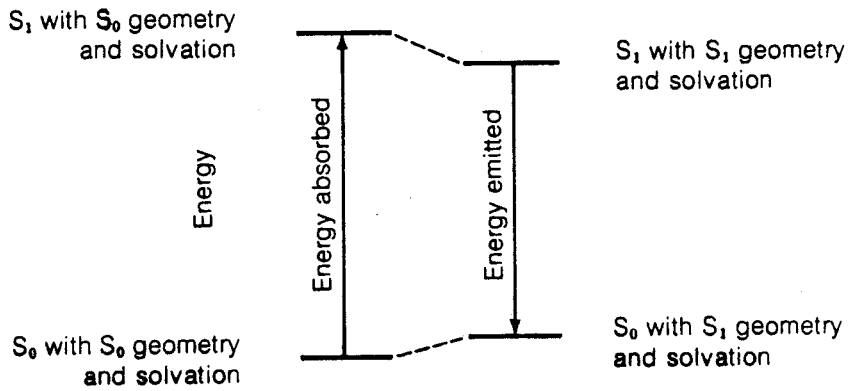

Figure 7 : Diagrammatic representation of the origin of the energy difference between absorption and emission processes.

2.3 Excited State Quenching

Fluorescence or phosphorescence intensities may be quenched by deactivation of the excited states that are responsible for the emission. Quenching processes are divided into two broad categories depending on the nature of the quenching. In dynamic quenching, interactions between the quencher and the potential luminescer take place during the lifetime of the excited state. This type of quenching is limited by the lifetime of the excited state and by the concentration of the quenching species. Static quenching is characterised by the formation of a complex between a potentially fluorescing molecule in its ground state with a quenching species. In the absence of the quencher the molecule would fluoresce, but together as a complex, no fluorescence is observed.

For dynamic quenching, the dependence of the relative quantum yield of fluorescence (Φ_o/Φ), upon quencher concentration Q may be derived from Stern-Volmer kinetics, and is given by

$$\Phi_o/\Phi = 1+k_q\tau_o[Q]$$

where Φ_o and Φ are the quantum yields in the absence and presence of the quencher, τ_o is the fluorescent lifetime of the molecule in the absence of the quencher, [Q] is the quencher concentration, and k_q is the bimolecular quenching rate constant.[54]

In protein studies the addition of external quenchers such as I^- has yielded both structural and dynamic information. Quenching by iodide is

thought to result from facilitated intersystem crossing from S_1 to T_1. This is promoted by spin-orbit coupling of the excited fluorophore and I^-, a process referred to as the heavy atom effect.[55]

2.4 Fluorescence Polarization

Polarization measurements provide a measure of the average angular displacement of the fluorophore that occurs between absorption and subsequent photon emission. Polarization results from the photoselection of fluorophores that have their dipole moments oriented parallel to the excitation light. Those molecules whose transition moment makes the smallest angle with the electric field vector of the exciting light absorb the greatest amount of light.

The degree of polarization, P, of the emission is defined by

$$P = (I_{II}-I_{\perp})/(I_{II}+I_{\perp})$$

where I_{II} and $I_{\perp}$ are emission intensities parallel and perpendicular to the plane of polarized excitation light (figure 8).[56] Maximum polarization values occur when molecules do not undergo rotational motions during their excited lifetime. If the absorption and emission transition moments are situated at an angle β with respect to one another, then the intrinsic polarization P_o, is denoted by

$$P_o=(3Cos^2\beta-1)/(Cos^2\beta+3)$$

For completely rigid molecules that do not interact with others, the maximum polarization in solution is 0.5, a value rarely attained because of rotational diffusion during the fluorescence lifetime. Polarization studies with proteins have yielded information pertaining to protein denaturation, protein-ligand association, and rotational diffusion rates.

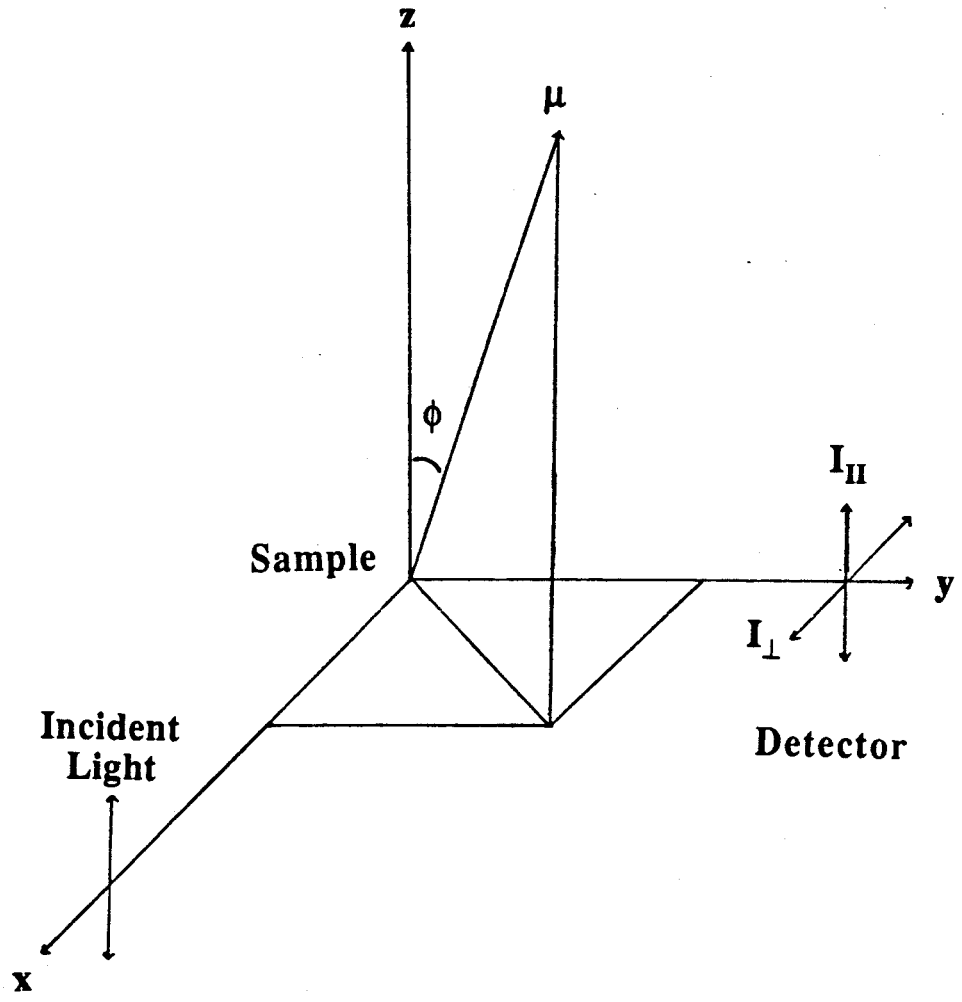

Figure 8 : Experimental arrangement for fluorescence polarization studies. Incident light polarized parallel to the Z axis interacts with μ, the absorption dipole moment of the fluorophore, while detection of the resulting emission occurs at 90° to the incident light.

2.5 Circular Dichroism

If a substance is optically active, then for each wavelength in its absorption band, it will display differential absorptions for left (L) and right (R) circularly polarised light. The L and R circularly polarised components pass through the optically active medium with different speeds and are differentially absorbed. Consequently, the electromagnetic waves exiting the medium will have different amplitudes and phases, which together produce a wave that is elliptically polarized.

Differential absorption is usually expressed in terms of the extinction coefficients for L and R circularly polarised waves, ε_L and ε_R, where $\Delta\varepsilon$, the circular dichroism, is

$$\Delta\varepsilon = \varepsilon_L - \varepsilon_R$$

Experimentally, $\Delta\varepsilon$ is usually measured, but for historical reasons the ellipticity (Ψ) is plotted, where Ψ is simply the arctangent of the ratio of the minor axis to the major axis of the ellipse that characterises the elliptically polarized light.[57,58] To eliminate the dependence on path length and on concentration the specific ellipticity, $[\Psi]$, for a given temperature and wavelength may be used. This quantity is defined as

$$[\Psi] = \Psi / l \cdot c$$

and expressed in units of $deg \cdot cm^2 \cdot dag^{-1}$, where l is the light path length in dm, and c is the sample concentration in $g \cdot cm^{-3}$.

For the purposes of comparison between compounds of different molecular weights the molar ellipticity, [θ], is used,

$$[\theta] = [\Psi] \cdot M / 100$$

where M is the molar mass of the optically active compound in $g \cdot mol^{-1}$, and [θ] is expressed in units of $deg \cdot cm^2 \cdot dmol^{-1}$. The relation between the circular dichroism and molar ellipticity is

$$[\theta] = 3300(\varepsilon_L - \varepsilon_R)$$

The constituents that give rise to a protein CD spectra are the asymmetric centres in the molecule, and the various specific arrangements that these centres attain in three-dimensional space. Absorptions due to the peptide backbone lie in the ultraviolet region, the strongest of which appear below 230 nm. Investigations of proteins with circular dichroism yields information about the fundamental optical properties of these molecules, which may then be used to ascertain secondary (2°) structure. Because of the strong contributions of protein 2° structure to CD spectra, chiroptical measurements are a convenient way of monitoring chemical and thermal denaturation of a protein.

In the simplest model, the three major 2° structures that absorb L and R circularly polarized light are the α-helix, the β-pleated sheet, and the random coil. The absorptions of these components are assumed to be additive, the sum of which constitutes a composite CD signal. The fractional composition of these three structures f_H, f_β, and f_R, in a protein may be

determined by the two following relations,

$$[\theta] = f_H X_H + f_\beta X_\beta + f_R X_R \quad \text{and} \quad \Sigma f_i = 1$$

where $[\theta]$ is the observed mean residual ellipticity, and X_H ,X_β, and X_R are the mean residual ellipticities of pure α-helical, β-pleated sheet, and random coil structures, respectively. Pioneering work by Greenfield and Fasman provided values for X_H ,X_β, and X_R by CD analysis of synthetic reference polypeptides that consisted entirely of only one of the three discussed 2° structures.[59] Alternatively, secondary structure may be estimated by comparisons with reference spectra based on proteins with known three dimensional structures.[60]

III. Objectives

The focus of research in our laboratory is actin and the regulation of actin filament assembly and disassembly. My objectives in studying horse plasma gelsolin were as follows:

1.(a) Preparation of a covalently modified, fluorescent conjugate of horse plasma gelsolin.

(b) Demonstration of structural and functional integrity of the modified gelsolin.

(c) Utilization of fluorescently labelled gelsolin to probe novel interactions.

2. Further investigation of the sulfhydryl environment on gelsolin using Cys conjugates previously characterised in our laboratory.

Chapter 2

MATERIALS AND METHODS

I. Protein Isolation and Purification

1.1 Purification of Actin

Actin was purified from an acetone-dried powder prepared from minced rabbit muscle tissue (Pel-Freez Biological) according to a procedure based on the method of Spudich and Watt.[61]

Initially, 10 grams of rabbit muscle powder was extracted with 200 mL of 2 mM Tris-HCl, 1 mM DTT, 0.2 mM ATP, and 0.2 mM $CaCl_2$, pH 7.6 (buffer A) for 30 minutes on ice. The extract was filtered through a double layer of cheesecloth, and the remaining solid residue re-extracted with an additional 100 mL of buffer A followed by another cheesecloth filtration. Both filtrates were combined and refiltered through Whatman #3 filter paper. The sample was clarified by centrifugation for 1 hour at 80 000 xg, after which the pellet was discarded. The remaining supernatant was made up to 150 mM KCl and 2 mM $MgCl_2$, and left undisturbed to polymerise overnight at 4°C. Solid KCl was then added to the F-actin solution to 0.8 M and gently stirred for 1.5 hours. Centrifugation for 3 hours at 80 000 xg pelleted the F-actin, while the supernatant was discarded. The translucent pellet was

resuspended in 30 mL of buffer A and converted back to G-actin by extensive dialysis against buffer A at 4°C. After dialysing for 3 days the G-actin was clarified by a final centrifugation at 80 000 xg for 3 hours, frozen in liquid nitrogen, and stored at -20°C until needed.

Concentrations of solutions containing G-actin were determined spectrophotometrically using an absorption coefficient at 290 nm of 0.63 mL mg^{-1} cm^{-1}.[62]

1.2 Purification of Gelsolin

Gelsolin was purified from frozen horse plasma by modification of a procedure described by Bryan.[28] Typically, 0.5 L of frozen horse plasma was thawed in the presence of the protease inhibitors leupeptin and pepstatin (100 µL of each stock solution at 2 mg mL^{-1} in H_2O and DMSO, respectively), and with phenylmethylsulfonyl fluoride (PMSF) added to 0.2 mM. The thawed plasma was dialysed at 4°C against three 10 L changes of 25 mM Tris-HCl and 0.5 mM $CaCl_2$, pH 7.5, over 3 days. Centrifugation at 10 000 xg for 15 minutes clarified the plasma, which was then adjusted to 35 mM NaCl and 1 mM NaN_3.

Initial fractionation of the plasma proteins was achieved with a batch anion exchange procedure. The dialysed plasma was added to approximately 2 L of settled DEAE Sephadex A-50 (Pharmacia) which had been equilibrated

against 50 mM NaCl, 25 mM Tris-HCl, 1 mM NaN_3, and 0.5 mM $CaCl_2$, pH 7.5. The mixture reacted for 2 hours at 4°C with occasional gentle stirring, after which the plasma lost its colour to the ion exchanger. The resultant slurry was filtered, the clear filtrate made up to 10 mM EDTA, and the pH adjusted to 7.8. The EDTA containing protein solution was applied at 1 mL min^{-1} to a 36 x 6 cm DEAE Sephadex A-50 column at 4°C, that had been previously equilibrated with 50 mM NaCl, 25 mM Tris-HCl, 1 mM NaN_3, and 0.1 mM EGTA, pH 7.8. After loading, the column was washed with two bed volumes of equilibration buffer, and the retained proteins eluted with a linear 50 to 300 mM NaCl gradient, also made up in equilibration buffer. Fractions were monitored for protein content by UV absorbance at 280 nm, and gelsolin localised in those fractions by polyacrylamide gel electrophoresis (PAGE) in the presence of sodium dodecyl sulfate (SDS) and 2-mercaptoethanol according to the method of Laemmli.[63] Fractions containing pure gelsolin were pooled and concentrated to approximately 1 mg mL^{-1} by ultrafiltration with a YM-30 membrane (Amicon).

On the occasions that gelsolin at this stage showed signs of contamination, an additional chromatographic step using Affi-Gel Blue (BioRad Laboratories) was implemented. The concentrated protein was dialysed at 4°C against 100 mM NaCl, 25 mM Tris-HCl, 1 mM EDTA, pH 8.0, and then applied at 1 mL min^{-1} to a 2.5 x 20 cm Affi-Gel Blue column that had been equilibrated with the same buffer. After a 2 bed volume

wash with equilibration buffer, gelsolin was eluted with a 0.1 to 2 M NaCl gradient. Biospecific elution of horse plasma gelsolin with ATP, according to the method of Ito *et al.* for human plasma gelsolin, was not achievable even at elevated ATP concentrations.[64]

Horse plasma gelsolin concentrations were determined spectrophotometrically using an extinction coefficient of 1.4 mL mg^{-1} cm^{-1} at 280 nm, as determined in this laboratory by Ruiz Silva and Burtnick.[65]

1.3 Purification of Tropomyosin

Skeletal and cardiac muscle tropomyosins were purified according to the protocol described by Smillie.[66] Essentially, tropomyosin was extracted from acetone-dried rabbit muscle powder with 1 M KCl at neutral pH, and purified by repeated cycles of isoelectric precipitation at pH 4.6, followed by ammonium sulfate fractionation at pH 7.0. At this stage low levels of contaminating troponin components and their proteolytic fragments were removed by chromatography on hydroxylapatite (BioRad Laboratories) using a 10 to 300 mM phosphate gradient.

1.4 Determination of Gelsolin Purity and Severing Activity

Gelsolin purity was assessed by electrophoresis on 10% polyacrylamide gels (BioRad Mini-Protean II) in the presence of SDS and 2-mercapto-

ethanol.[63] Purified horse plasma gelsolin produced a single Coomassie stained band with a molecular mass of 90 000 daltons.

Viscosity measurements were conducted to determine the actin severing activity of gelsolin. Gelsolin was added to 25 μM actin solutions in 150 mM KCl, 2 mM Tris-HCl, 1 mM DTT, 0.2 mM $CaCl_2$, and 0.2 mM ATP, pH 7.6, in amounts yielding an actin to gelsolin mole ratio of 50:1. After 60 minutes of incubation, viscosity measurements were made with a Cannon-Manning semi-micro viscometer (size 100) in a thermostatically controlled water bath at 27°C. Each 1 mL sample was analysed 3 consecutive times, yielding very reproducible flow times between repetitive runs. The flow time for buffer was 103.5 seconds with a standard deviation of ± 0.4 seconds.

II. Chemical Modification of Gelsolin

2.1 Primary Amine Modification with Fluorescein

Gelsolin was labelled with the amine selective reagent fluorescein-5-isothiocyanate (FITC isomer 1, Molecular Probes) by modification of the procedure given for G-actin.[67] Relative to sulfonyl chlorides which are highly reactive and succinimidyl esters which are slow to react, isothiocyanates are of intermediate reactivity towards nucleophilic attack. Aliphatic amines such as lysine react with isothiocyanates to form thioureas which are highly stable in water. This reaction occurs best above pH 8.5 where a limited fraction of amines are unprotonated and reactive.

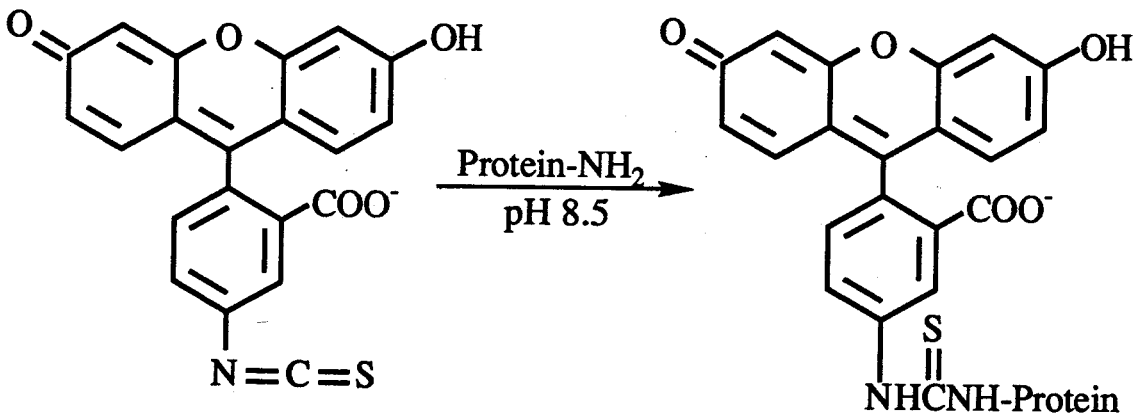

FITC **Thiourea**

The protein was initially dialysed against 150 mM KCl, 50 mM Hepes, and 1 mM EDTA, pH 8.5. FITC, approximately 2 mg dissolved in a minimal amount of 0.1 M NaOH, was added to a stirring gelsolin solution and allowed to react for 24 hours at 4°C in a dark environment. All subsequent dialysis procedures with modified gelsolins were conducted in the dark to prevent photobleaching, and at 4°C to enhance protein stability. Unreacted FITC was removed by an initial 24 hour dialysis against 150 mM KCl, 25 mM Tris-HCl, and 1 mM EDTA, pH 8.0. The FITC-labelled gelsolin was gel filtered through a 1.3 x 45 cm Bio-Gel P-2 column (BioRad Laboratories) which had been previously equilibrated with 150 mM KCl, 25 mM Tris-HCl, and 1 mM EDTA, pH 8.0. Fractions yielding fluorescence when viewed with a hand-held UV lamp were pooled and concentrated with Centricon-30 micro-concentrators (Amicon). Further dialysis in the above buffer was conducted over the next 2 days with a change of buffer on each day.

2.2 Primary Amine Modification with Benzophenone

The procedure for labelling gelsolin with benzophenone-4-isothio-cyanate (BITC, Molecular Probes) was similar to the FITC-labelling protocol. Approximately 2 mg of BITC dissolved in a minimal amount of N,N-dimethylformamide (DMF) was added to gelsolin that had been dialysing in 150 mM KCl, 50 mM Hepes, and 1 mM EDTA, pH 8.5. The reaction mixture was gently stirred for 24 hours in the dark at 4°C. Microcentrifugation for

15 minutes removed precipitated BITC, and extensive dialysis for 3 days with 3 changes of 25 mM Tris-HCl, and 1 mM EDTA, pH 8.0 quenched any unreacted BITC.

2.3 Sulfhydryl Modification with Acrylodan

The fluorescent probe 6-acryloyl-2-dimethylaminonaphthalene (acrylodan or ACR, Molecular Probes) was used to S-alkylate gelsolin cysteine amino acids. This α,β-unsaturated fluorophore reacts efficiently and selectively with thiols at pH 8.0 via a Michael-type mechanism, yielding a 1,4-addition product. Acrylodan adducts have strongly environment-dependent fluorescence that is sensitive to ligand binding.

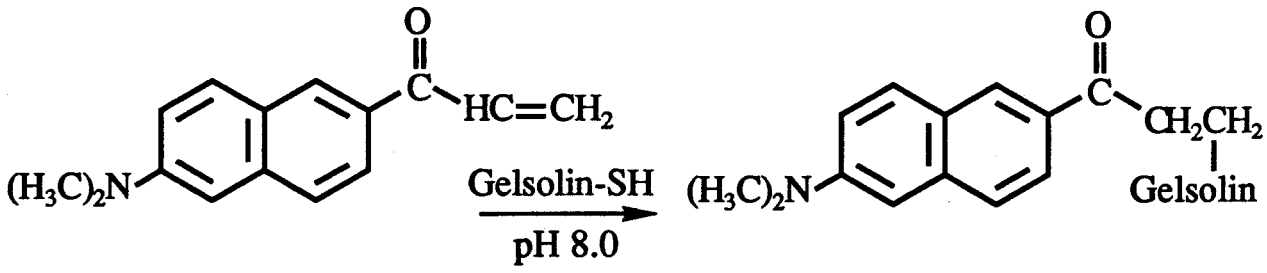

Acrylodan **ACR-Gelsolin**

Gelsolin was initially dialysed against 150 mM KCl, 25 mM Tris-HCl, 1 mM EDTA, and 1 mM DTT, pH 8.0 for 24 hours at 4°C. DTT, which promotes Cys thiol reduction, was removed prior to reaction by a 4 hour dialysis in the above buffer without DTT. To a stirred gelsolin solution, 2 mg of acrylodan dissolved in a minimal amount of DMF was added. The reaction was conducted for 24 hours in the dark and at 4°C. Insoluble acrylodan was removed by centrifugation at 15 000 xg for 15 minutes, and the supernatant dialysed against 150 mM KCl, 25 mM Tris-HCl, 1 mM EDTA, and 1 mM DTT, pH 8.0 for 24 hours. Acrylodan-labelled gelsolin was gel filtered and concentrated as previoulsy described for FITC-labelled gelsolin using 150 mM KCl, 25 mM Tris-HCl, 1 mM EDTA, and 1 mM DTT, pH 8.0, for the running buffer.

In an attempt to increase the extent of acrylodan incorporation, the labelling reaction was carried out in 6 M guanidine-HCl, and stirred for 24 hours at room temperature. Renaturation of acrylodan-labelled gelsolin was attempted by extensive dialysis against 150 mM KCl, 25 mM Tris-HCl, 1 mM EDTA, and 1 mM DTT, pH 8.0.

2.4 Sulfhydryl Modification with Pyrene

Iodoacetamides are common reagents for thiol modification in the physiological pH range. The nucleophilic substitution reaction at or below room temperature usually proceeds rapidly with the production of very stable

thioethers. N-(1-pyrene)iodoacetamide (PIA, Molecular Probes), another thiol selective fluorescent reagent, was the haloacetamide utilised to modify gelsolin.

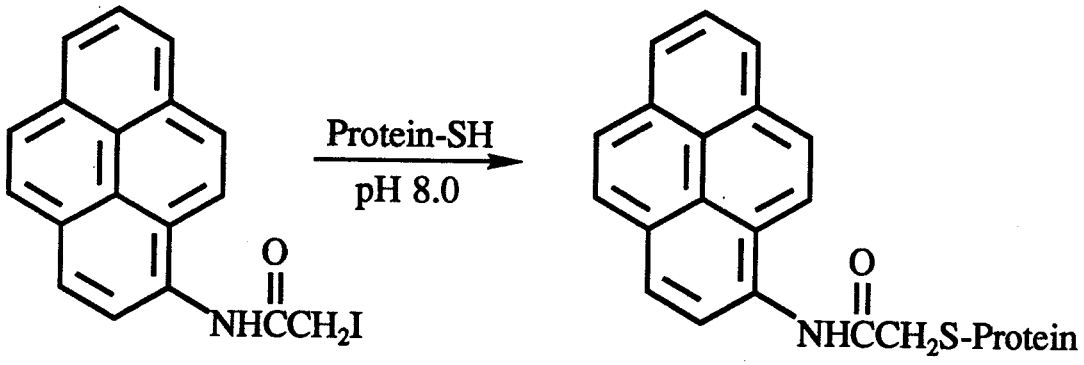

Treatment of gelsolin with PIA was essentially identical to that of acrylodan. The protein was initially reduced in 150 mM KCl, 25 mM Tris-HCl, 1 mM EDTA, and 1 mM DTT, pH 8.0. for a 24 hour period. To minimise unproductive reaction with DTT, a 4 hour dialysis prior to reaction was conducted against the above buffer minus the DTT. Precipitated PIA was removed by centrifugation at 15 000 xg for 15 minutes, followed by extensive dialysis against 150 mM KCl, 25 mM Tris-HCl, 1 mM EDTA, and 1 mM DTT, pH 8.0. Guanidine-HCl was also employed to increase the extent of alkylation with PIA. Labelling conditions were similar to those for the native protein, but guanidine-HCl was added to 6 M and the reaction conducted at room temperature.

2.5 Degree of Labelling

The average number of fluorophores incorporated into the gelsolin molecule was determined by independent measurements of fluorophore and protein concentrations.

$$\text{Degree of Labelling} = \frac{[\text{ Fluorophore }]}{[\text{ Gelsolin }]}$$

The gelsolin concentration was determined by the BioRad microassay which is based on the observation that the absorbance maximum of Coomassie Brilliant Blue G-250 shifts from 465 nm to 595 nm in protein solutions.[68] Fluorescent probe concentrations were estimated spectrophotometrically using published molar extinction coefficients. For FITC the molar extinction coefficient at 493 nm is 74 500 M^{-1} cm^{-1}, while for ACR the value is 12 900 M^{-1} cm^{-1} at 360 nm.[69,70] Similarly, PIA content was estimated using a value at 344 nm of 22 000 M^{-1} cm^{-1}.[71]

2.6 Determination of Gelsolin Sulfhydryl Content

To estimate the number of thiol groups that should be accessible to ACR and PIA, Ellman's assay using 5,5'-dithiobis(2-nitrobenzoic acid) (DTNB) was carried out on gelsolin in both native and denaturing conditions.[72] Standard curves were prepared by monitoring absorbances at

412 nm two minutes after the addition of stock DTNB to freshly prepared, separate solutions of DTT, 2-mercaptoethanol, and glutathione. All optical density measurements were conducted against a blank containing a standard amount of DTNB. Gelsolin-containing solutions in 100 mM potassium phosphate or in buffered 6M guanidine-HCl were assayed in a manner identical to the standards. Denatured gelsolin showed rapid colour development within 2 minutes, but native gelsolin required incubation times up to 90 minutes. At such times further absorbance changes at 412 nm were no longer detected.

III. Limited Proteolytic Digestion and Affinity Chromatography

3.1 Chymotryptic Digestion of ACR and FITC-labelled Gelsolins

Acrylodan-labelled gelsolin at approximately 0.4 mg mL^{-1} and FITC-labelled gelsolin at 0.65 mg mL^{-1} were digested with porcine pancreatic α-chymotrypsin (Type VII, Sigma) essentially as described by Kwiatkowski *et al.*[73] The labelled proteins were dialysed in 25 mM Tris-HCl and 1 mM EDTA, pH 8.0. $CaCl_2$ was then added to 2 mM, followed by the enzyme at a weight ratio to the labelled proteins of 1 to 100. Prior to its use, the enzyme had been dissolved in protein dialysis buffer and filtered through a 0.45 μm filter (Millipore). The reaction mixtures were incubated for up to 30 minutes at room temperature. At various times, aliquots of the digest were removed and the reaction quenched by the addition of PMSF (dissolved in ethanol) to 0.5 mM and EDTA to 2 mM. Digestion products were analysed on 12.5% polyacrylamide gels in the presence of SDS and 2-mercaptoethanol.

3.2 Tropomyosin-Agarose Affinity Chromatography

Rabbit skeletal tropomyosin (S-TM) was coupled to Affi-Gel-15 (BioRad Laboratories) according to the supplier's recommended procedure.

S-TM was dialysed against 100 mM Mops, pH 7.5 and added proportionately to the N-hydroxysuccinimide activated matrix; 35 mg of S-TM were added per mL of gel. The suspension was gently agitated overnight at room temperature on a mechanical rocker. The coupled affinity matrix was poured into a 5 mL measuring pipet, and extensively washed with 25 mM Tris-HCl, and 1 mM EDTA, pH 8.0 to displace any unreacted N-hydroxysuccinimide groups. Prior to use, the column was equilibrated with 25 mM Tris-HCl, pH 8.0 and either 1 mM EDTA or 1 mM $CaCl_2$. Gelsolin labelled with either FITC or ACR was applied until fluorescence appeared in the column eluant, indicating saturation of the TM-agarose matrix. The column was then extensively washed with equilibration buffer until no fluorescence was detected in the eluant. The adhered gelsolin was removed from the S-TM affinity matrix with a 0 to 500 mM KCl gradient made up in equilibration buffer. Fractions were collected in 2 mL volumes and monitored for protein content by fluorescence. The identities of the eluted proteins were confirmed to be FITC and ACR-labelled gelsolins by SDS-polyacrylamide electrophoresis.

IV. Optical Techniques

4.1 Absorbance Measurements

Proteins were detected and their concentrations determined at various stages during and after the purification procedure with a Lambda 4B UV/Vis Spectrophotometer (Perkin Elmer). The same instrument was used to conduct the BioRad and Ellman colorimetric assays.

4.2 Fluorescence Measurements

Fluorescence studies were performed with a LS-5B Luminescence Spectrometer equipped with a 7500 series computer (Perkin-Elmer) and a circulating water bath (Haake). Polarization values were obtained using a semi-automatic polarization accessory and PTPOL software (Perkin-Elmer). Included in the PTPOL software is a wavelength-dependent gratings correction factor. All polarization values are an average of three independent measurements, with typical standard deviations of $\pm$ 0.002.

4.3 Circular Dichroism

A Jasco J-20 spectropolarimeter equipped with a photoelastic modulator and modified for computer control and data acquisition (Landis Instruments)

was used for circular dichroism measurements. The cell and optical chambers were purged with nitrogen, and the cell chamber was thermostatically controlled with a Grant circulating water bath. Thermal denaturation studies were performed at a fixed wavelength of 215 nm, allowing an equilibration time of 15 minutes at each new temperature setting.

4.4 Photochemical Crosslinking

Rabbit cardiac tropomyosin in 25 mM Tris-HCl, pH 8.0 and either 1 mM EDTA or 1 mM $CaCl_2$ was mixed with solutions of BITC-labelled gelsolin. Samples of labelled gelsolin were dialysed extensively against either of the two above mentioned buffers, creating a plus and minus calcium environment. The solutions were placed into a 1 cm jacketed quartz cuvet (Hellma) and cooled to 4°C using a Haake circulating water bath. A 200 W Hg arc lamp (Osram) and a Corning #7-54 bandpass filter that excludes light below 250 and above 400 nm were used in conducting the photoactivation. At various times during the reaction, aliquots of the mixture were removed and examined by SDS-polyacrylamide gel electrophoresis.

Upon photoexcitation, the benzophenone moiety on labelled gelsolin converts to a triplet diradical that may participate in photochemical reactions. The diradical abstracts a hydrogen atom from tropomyosin to form a tropomyosin radical and a photoreduced benzophenone species. Radical recombination between the tropomyosin and the benzophenone species results

in the formation of various high molecular weight products.

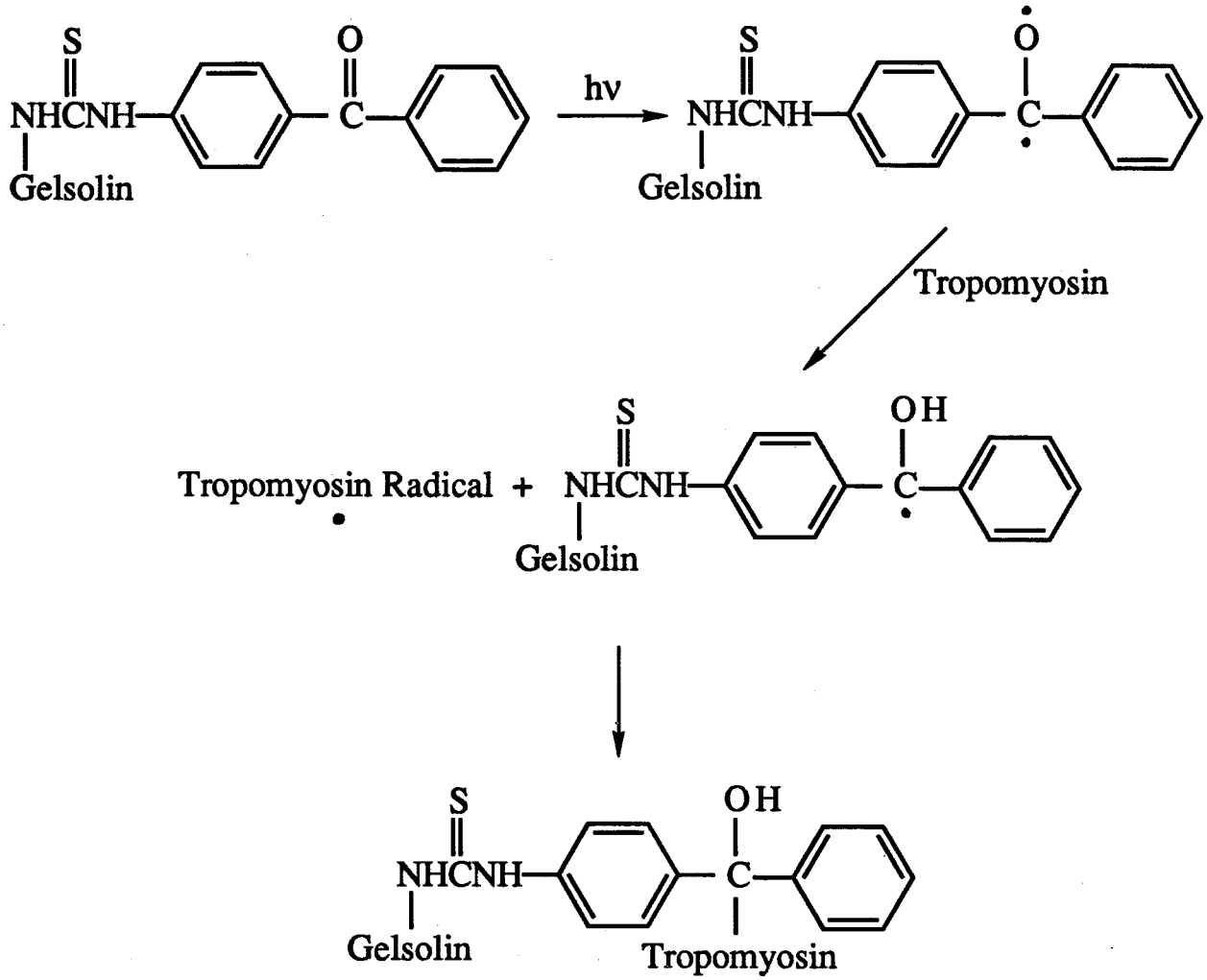

Crosslinked Product

Chapter 3

RESULTS AND DISCUSSION

I. Modification of Gelsolin with FITC

1.1 General Characterisation

The reaction of fluorescein-5-isothiocyanate with gelsolin produced a fluorescently derivatised protein that contains 4 to 6 modified primary amine groups. Specifically, the level of incorporation of FITC into gelsolin was determined to be 4.8 ± 0.6 (mean ± standard deviation) based upon 4 labelling experiments. Since horse plasma gelsolin contains 44 possible modification sites as determined by the Lys amino acid content (excluding the NH_2 terminal), a degree of labelling of 4.8 suggests that most of the Lys residues are inaccessible to FITC.[65] The Lys residues that were derivatised are probably located on regions of polypeptide segments that expose themselves to solvent, thereby minimising steric constraints between the isothiocyanate and the primary amine groups. FITC-labelled gelsolin showed a single fluorescent band when viewed under UV light and then a single Coomassie Blue stained band on 10% SDS-PAGE gels. These observations establish that FITC binds to gelsolin covalently, and that the labelling reaction conditions do not induce peptide bond cleavage.

To assess FITC-labelled gelsolin's activity with respect to actin severing, a series of viscosity measurements was undertaken (Table 1). Under the polymerising conditions of 150 mM KCl in buffer A, solutions of 25 μM actin exhibit a relative viscosity of 1.49, a value that decreases to 1.04 in non-polymerising buffer A. Increasing amounts of FITC-labelled gelsolin added to actin solutions at 25 μM final concentration correlate with a relative viscosity decrease, yielding a value virtually identical to that of G-actin at a 1:10 mole ratio. Similarly, at a 1:50 mole ratio the relative viscosities for both labelled (1.12) and unlabelled (1.09) gelsolins compare favourably, indicating that the F-actin severing activity has not been impaired as a consequence of labelling.

Table 1 : Viscosity Measurements with FITC-labelled Gelsolin

Sample	Relative Viscosity
1:200	1.24
1:150	1.19
1:100	1.16
1:50	1.12
1:25	1.09
1:10	1.05
F-actin	1.49
G-actin	1.04
Gelsolin/actin (1:50)	1.09
Buffer	1.00

Each 1 mL sample contained 150 mM KCl in buffer A, pH 7.6 at 27°C. Actin in buffer A was added to samples to a final concentration of 25 μM, and left undisturbed for 60 minutes. Ratios listed represent mole ratios of FITC-labelled gelsolin to actin. Relative viscosities were calculated by dividing the flow time of each sample by the flow time of 150 mM KCl in buffer A.

In the 400 nm to 520 nm range, the absorption spectrum of FITC-labelled gelsolin shows a wide peak with the absorption maximum located at 499 nm (figure 9). Upon excitation at 490 nm a single broad band emission typical of fluorescein is observed, with the maximum intensity centred around 520 nm. Similar emission maxima are observed with FITC-labelled actin (517 nm), and with FITC-labelled cytochrome P450 at approximately 523 nm.[67,69] Since FITC-labelled gelsolin absorbs strongly in a wide range around 500 nm, an excitation wavelength of 490 nm, rather than 499 nm, was used to prevent scatter contributions to the observed fluorescence.

At near physiological ionic conditions, the emission intensity and wavelength maximum of FITC-labelled gelsolin is unaffected by the presence of calcium ions (figure 10). However, in lower ionic strength solutions the emission intensity increases approximately 25% upon the addition of Ca^{+2}. Whether or not this fluorescence increase is a consequence of a calcium induced conformational change remains to be determined. Since fluorescein emission is known to depend highly upon pH and on the solvent's dielectric constant, an increased exposure of labelled gelsolin's fluorescein groups to aqueous solvent at pH 8.0 should increase the fluorescence intensity.[74] For adequate emission, fluorescein must be used at a pH above its pKa of approximately 6.4, and in solvents with high dielectric constants. Fluorescein itself is only slightly fluorescent in alcoholic solutions, with the fluorescence disappearing upon replacing the alcohol with diethyl ether. At higher ionic

a

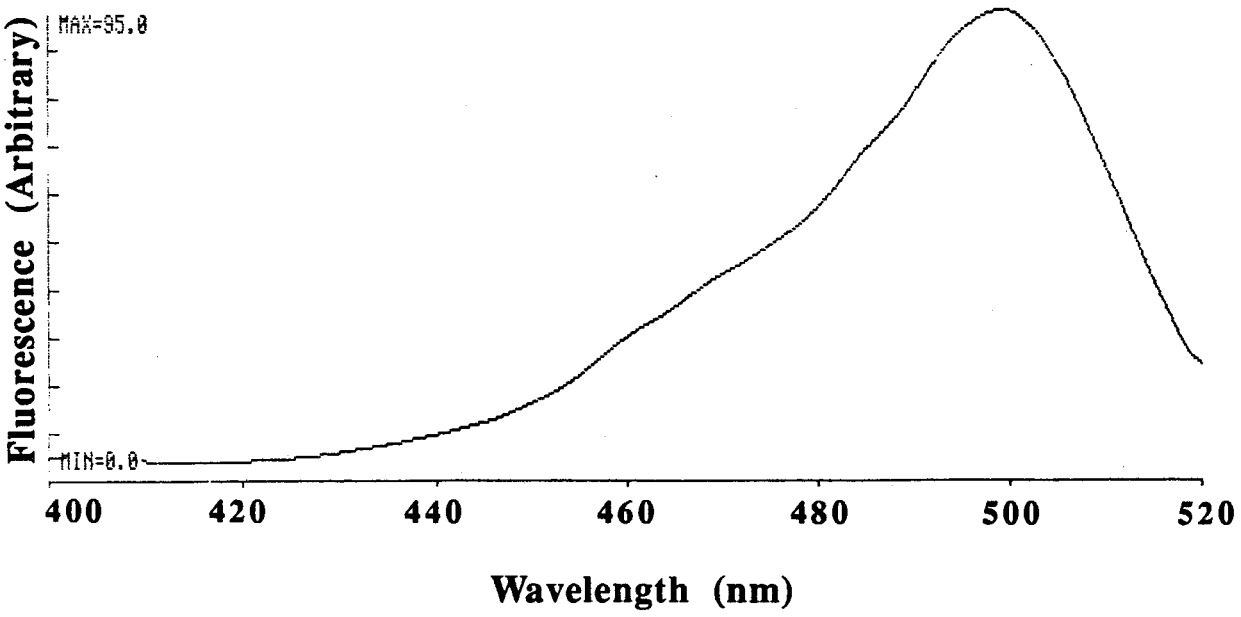

b

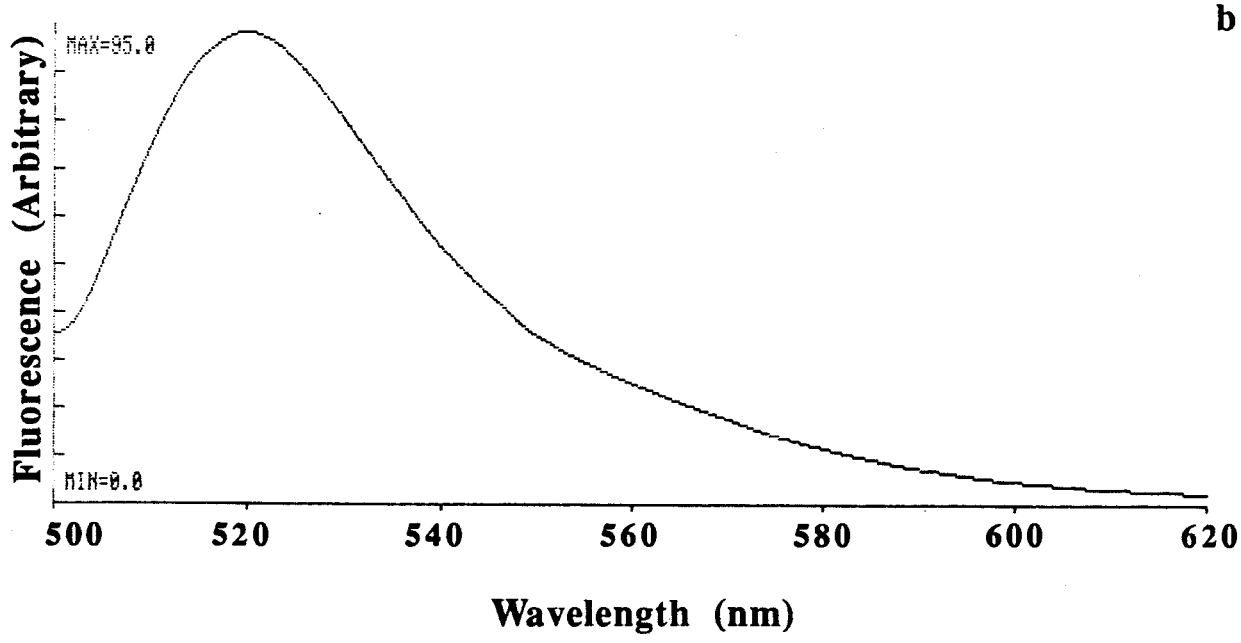

Figure 9 : Excitation (a) and emission (b) spectra of 0.5 μM FITC-labelled gelsolin in 150 mM KCl, 25 mM Tris-HCl, and 1 mM EDTA, pH 8.0. The emission wavelength was 520 nm in (a), and the excitation wavelength was 490 nm in (b).

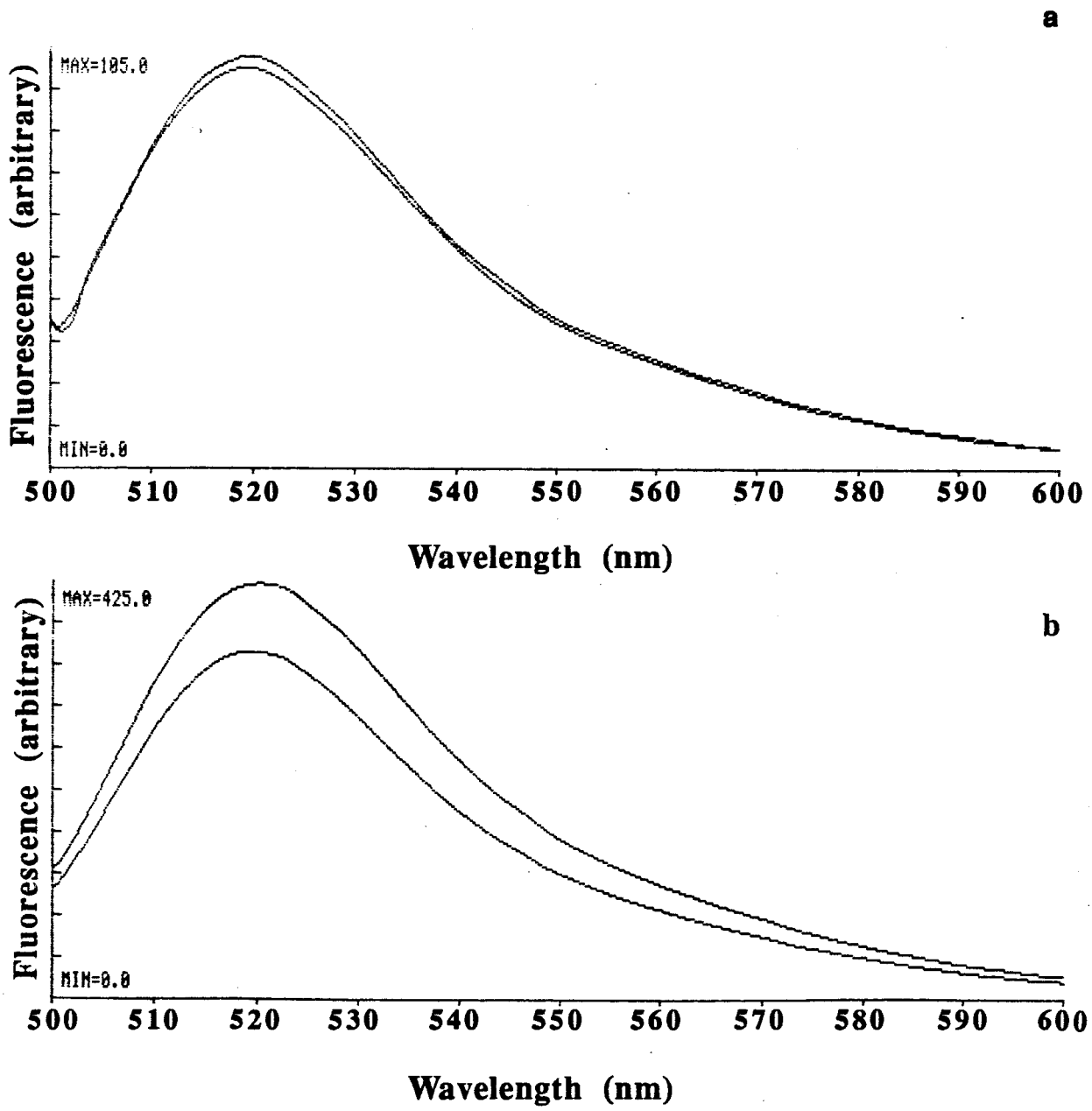

Figure 10 : Effect of calcium on the emission of FITC-labelled gelsolin. In (a), the emission of 0.5 μM labelled gelsolin was recorded in 150 mM KCl, 25 mM Tris-HCl and either 1 mM EDTA or 1 mM $CaCl_2$, pH 8.0. Part (b) was similar to (a) above, but the experiment was conducted in the absence of KCl. In both parts, the upper emission curves are those obtained in the presence of calcium. The excitation was at 490 nm, and the temperature set at 25°C for all scans.

strengths, the effects of protein surface charges diminish, lessening their contributions to the overall protein conformation. In lower ionic strength solutions, the binding of two Ca^{+2} ions will alter gelsolin's surface charge, which may then lead to a conformational change. A change in gelsolin's surface charge properties upon binding Ca^{+2} has been reported by Doi *et al.*, who found that the elution volume for gelsolin bound to a DEAE ion-exchange matrix altered drastically depending on the amount of free Ca^{+2} present in the medium.[75]

Bimolecular fluorescence quenching with iodide shows that the quenching efficiency is greater in the presence of micromolar calcium than in its absence (figure 11). The availability of this divalent cation increases the exposure of some, if not all, of the fluorescent probes to the surrounding solvent, resulting in a 20% greater quenching efficiency at 0.5 M KI. An additional contributing factor to the greater degree of quenching in calcium is a charge effect. The approach of negatively charged I^- will be hindered by negative charges residing on gelsolin's surface. Calcium bound to gelsolin diminishes negative surface charge and thus facilitates additional quenching. A further increase of the availability of fluorescein moieties to iodide was achieved by protein denaturation in 6 M guanidine-HCl (figure 12). This treatment pulls apart protein 2° and 3° structure, thereby increasing iodide's accessibility to the fluorescein groups. The large fluorescence decrease upon denaturation indicates that some of the fluorescein groups of intact FITC-

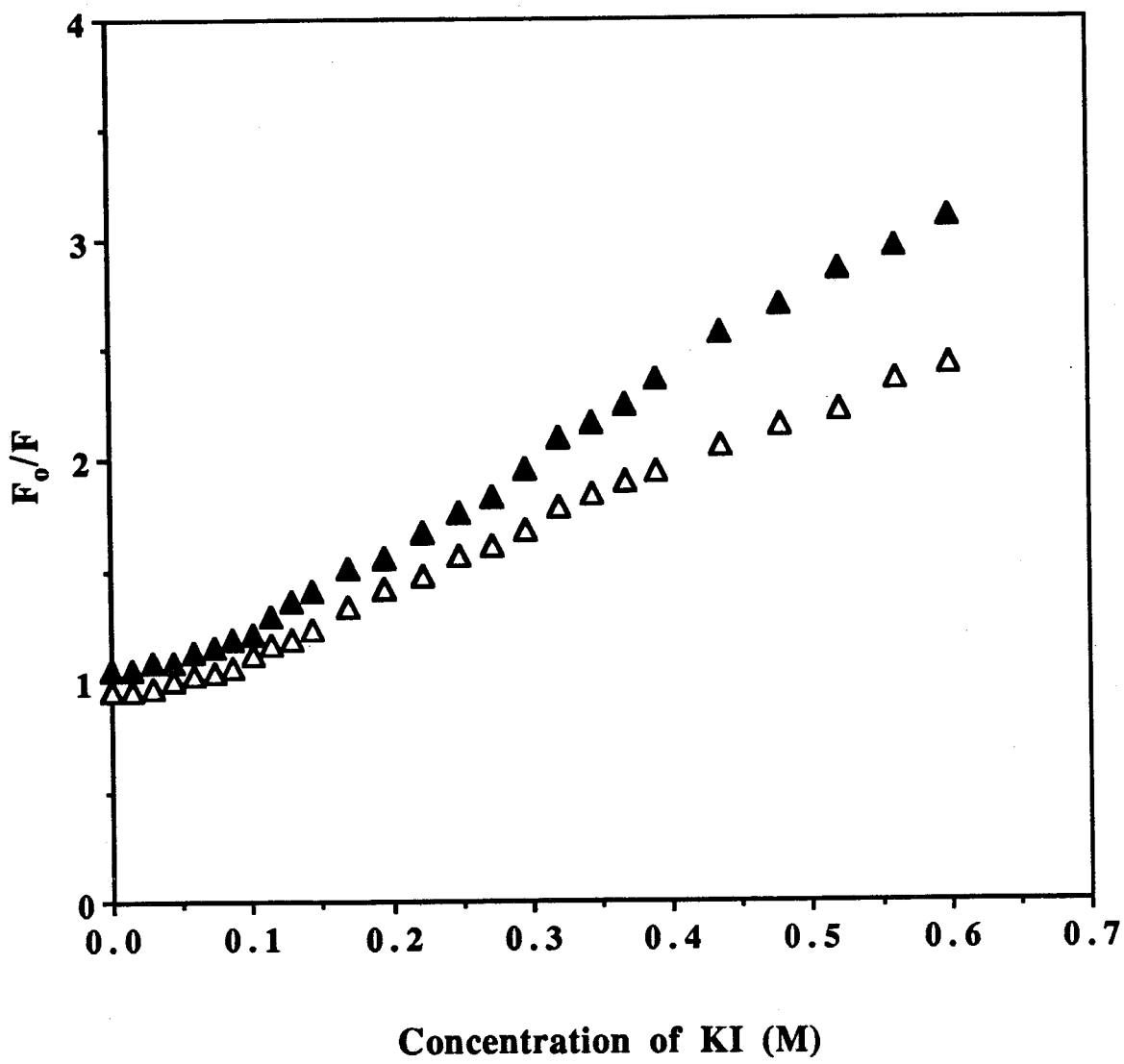

Figure 11 : Iodide quenching of FITC-labelled gelsolin in the presence and absence of calcium. Separate samples of 0.5 μM labelled gelsolin in 150 mM KCl, 25 mM Tris-HCl, and 1 mM EDTA, pH 8.0, at 25°C were titrated with KCl and KI to yield F_o and F values, respectively (Δ). Another set of samples containing 1 mM $CaCl_2$ instead of EDTA were treated in an identical manner (▲). Excitation and emission wavelengths, respectively, were 490 nm and 520 nm in all cases.

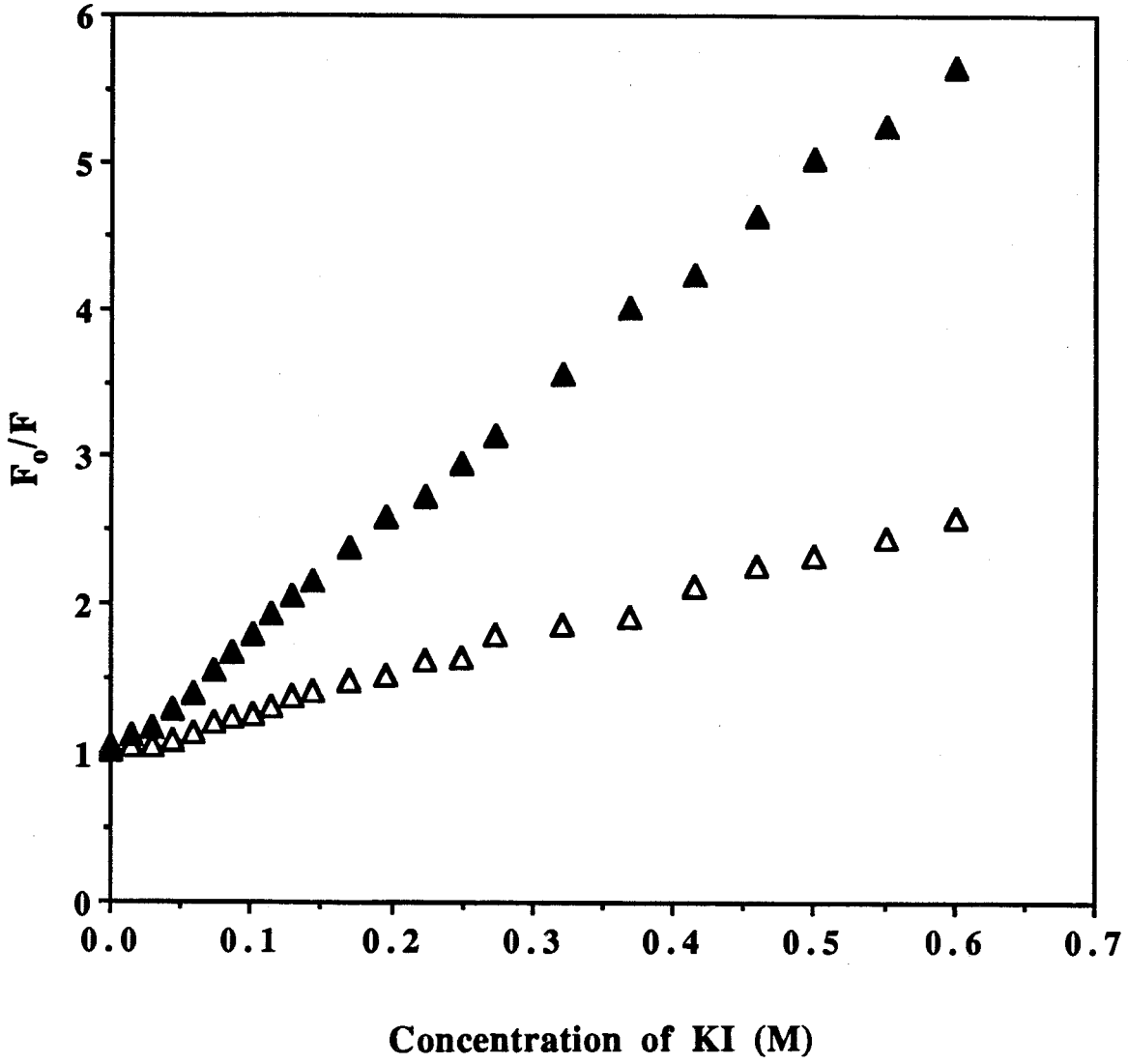

Figure 12 : Iodide quenching of 0.5 μM FITC-labelled gelsolin in both native and denaturing conditions. Titration under native conditions was conducted in 150 mM KCl, 25 mM Tris-HCl, and 1 mM EDTA, pH 8.0, at 25°C (Δ), while 6 M guanidine-HCl in an otherwise identical buffer was used to denature the protein (▲). F_o and F values were obtained as described in figure 11. Excitation was at 490 nm and emission at 520 nm.

labelled gelsolin are protected from the surrounding iodide rich solvent. In these quenching titrations, F values represent emission intensities obtained by titration with KI, while F_o values are those obtained by a KCl titration. The latter treatment serves to simultaneously correct for dilution effects and ionic strength changes.

A direct titration of FITC-labelled gelsolin with both Ca^{+2} and Mg^{+2} in EDTA containing buffer further demonstrates gelsolin's ability to bind calcium (figure 13). The titration with Mg^{+2} behaved similarly to a titration conducted with buffer. Addition of Ca^{+2} to the labelled protein yielded results similar to the Mg^{+2} case up to the EDTA equivalence point. Upon saturating all the available EDTA binding sites, the Ca^{+2} ions bind to gelsolin causing the fluorescence intensity to increase. These results concur with the emission spectra obtained in calcium deficient and calcium rich environments.

When viewed under UV light prior to staining, FITC-labelled gelsolin run on SDS-PAGE gels appears as a single fluorescent band. Limited proteolytic cleavage with α-chymotrypsin at a 1 : 100 enzyme to protein weight ratio produces fluorescent fragments that span the entire gelsolin peptide sequence (figure 14). Labelled gelsolin is rapidly cleaved into two major fragments that correspond to both the NH_2 and the COOH terminal domains.[31] Separation of these two fragments was not achieved on the gel at the loading level employed, as both bands co-migrated to a position that matches the 45 000 dalton molecular mass ovalbumin standard. At longer

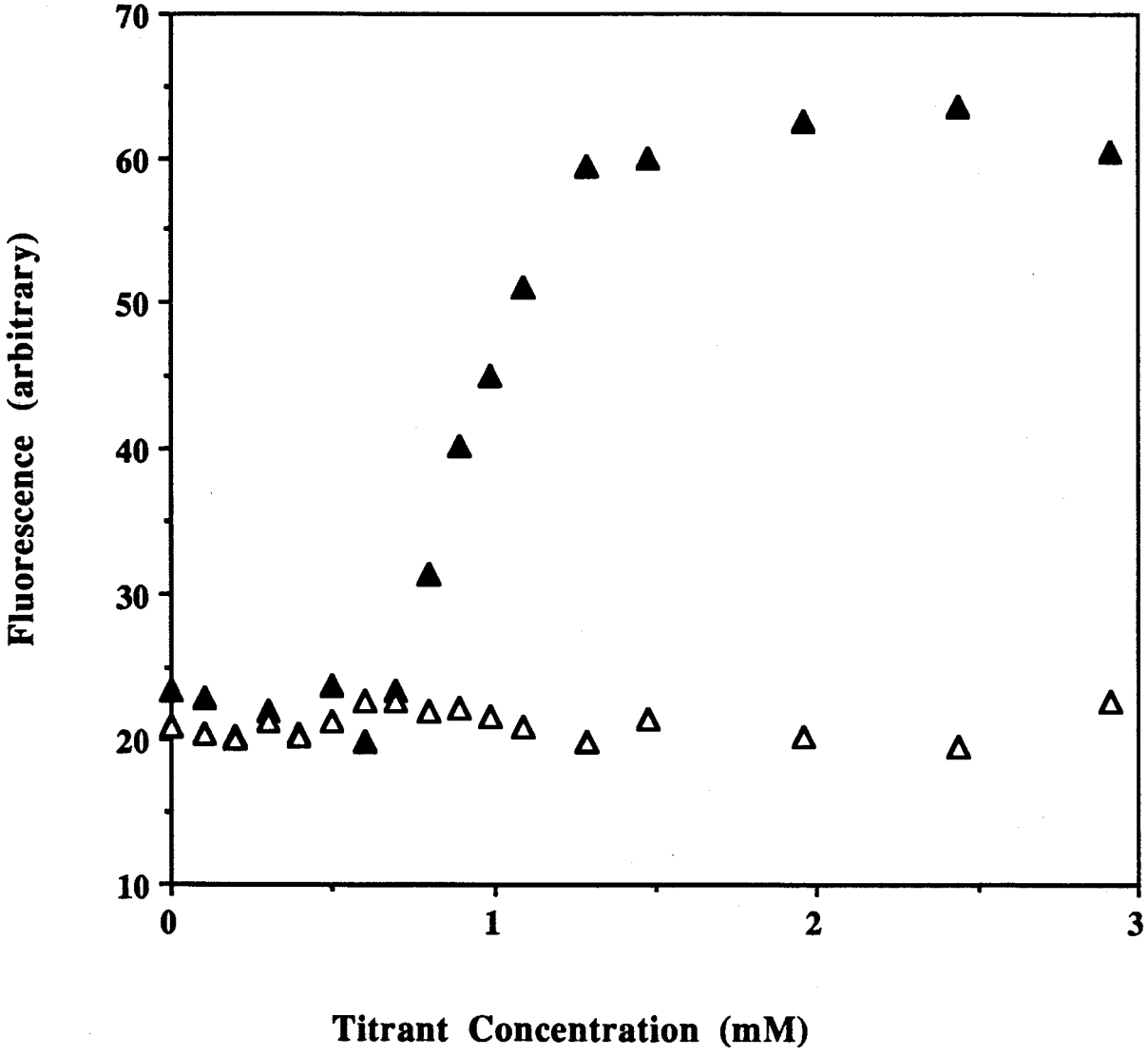

Figure 13 : Titration of FITC-labelled gelsolin with Ca^{+2} and Mg^{+2}. Fluorescein modified gelsolin at 0.25 μM in 150 mM KCl, 25 mM Tris-HCl, and 1 mM EDTA, pH 8.0 at 25°C was titrated with Ca^{+2} (▲), Mg^{+2} (Δ), and with buffer. The fluorescence readings of the Ca^{+2} and Mg^{+2} titrations were modified by subtracting the buffer titration readings. In all titrations, the excitation was set at 490 nm and the emission monitored at 520 nm.

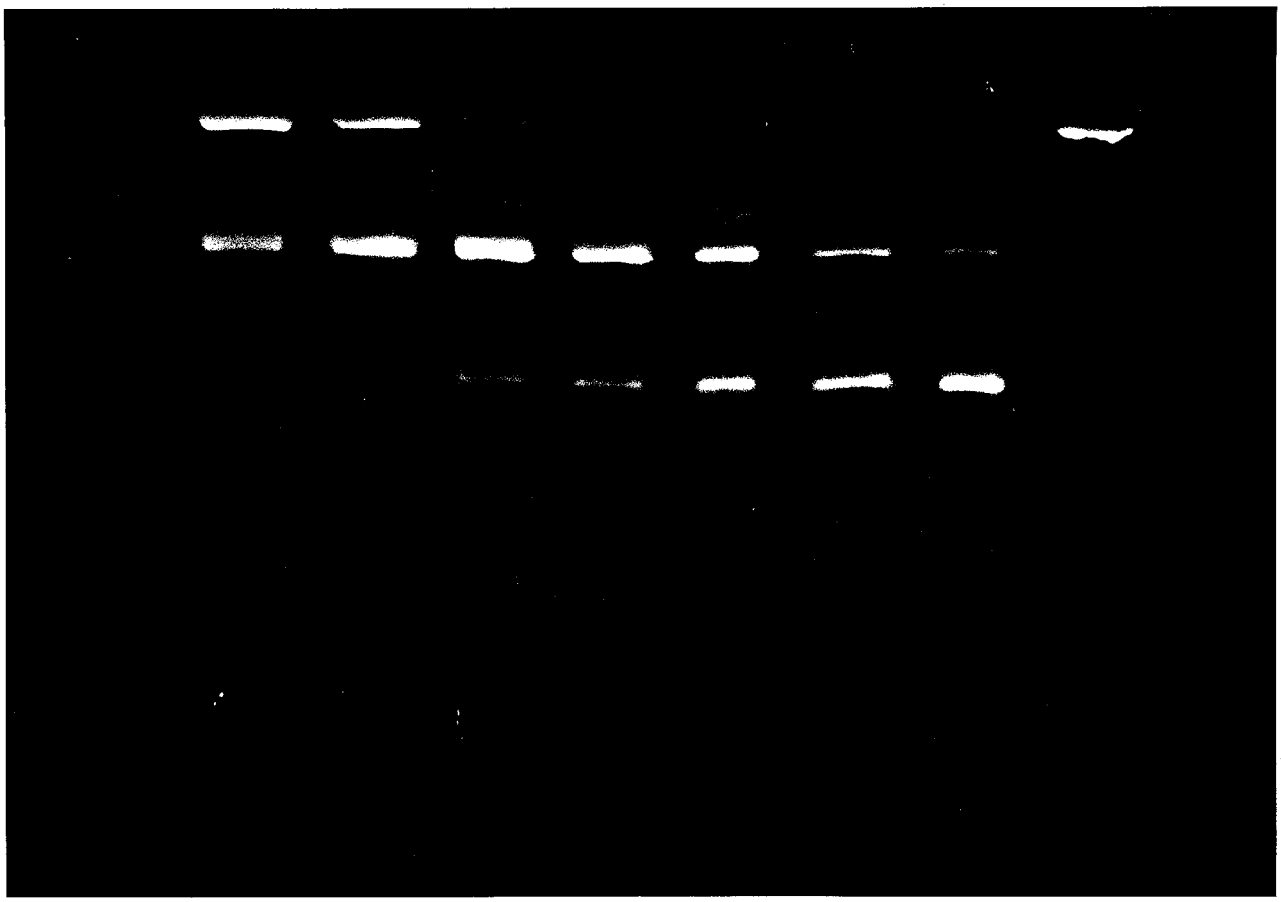

Figure 14 : Limited proteolytic cleavage of FITC-labelled gelsolin digested with α-chymotrypsin, and viewed under UV light prior to staining. Starting from the left, lanes 1 through 7 represent digestion times of 0.5, 1, 3, 5, 10, 20 and 30 minutes. Undigested FITC-gelsolin is shown in lane 8. Electrophoresis was conducted on 12.5% PAGE gels in the presence of SDS and 2-mercaptoethanol.

digestion times the large N-terminal segment breaks down to a couple of smaller fragments that have molecular masses of approximately 31 kDa and 15 kDa. The Coomassie stained gel of the same digest reveals a banding pattern similar to that obtained for human plasma gelsolin (figure 15).[31,73]

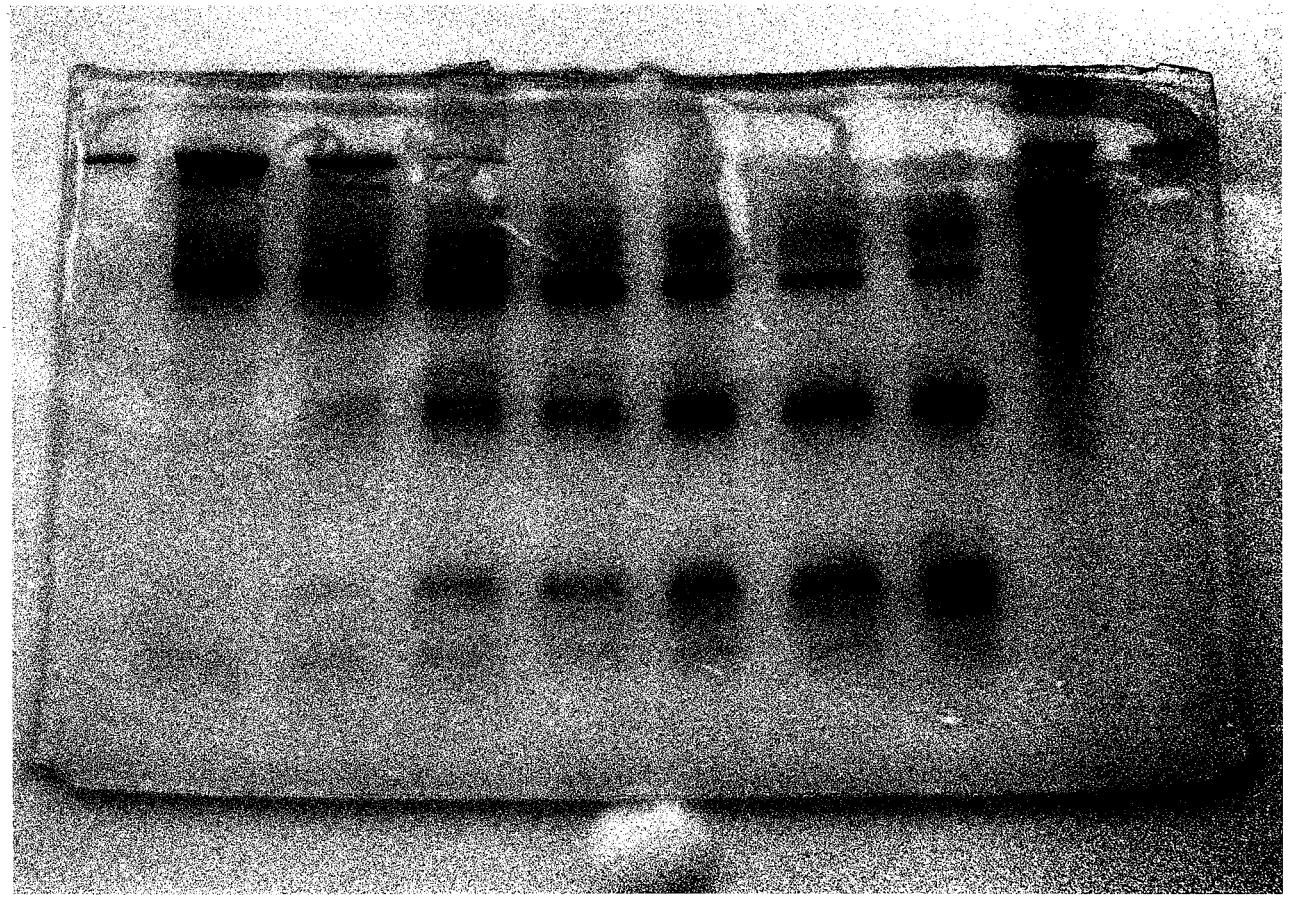

Figure 15 : SDS-polyacrylamide gel electrophoresis of the chymotryptic digest of FITC-labelled gelsolin viewed after Coomassie staining. Lane contents 2 to 8 in this gel are identical with lanes 1 to 7 of figure 14. Unlabelled gelsolin appears in lanes 1 and 10, and FITC-gelsolin, bovine serum albumin and ovalbumin (from top to bottom) in lane 9.

1.2 Interactions with Actin

Actin interactions with FITC-labelled gelsolin were monitored by an actin titration and by fluorescence polarization. To a pair of solutions of 0.5 μM FITC-labelled gelsolin in 150 mM KCl, 25 mM Tris-HCl, and either 1 mM EDTA or 1 mM $CaCl_2$, pH 8.0, aliquots of a stock actin solution were added. When excited at 490 nm, the fluorescence emission intensity at 520 nm increased only in the presence of calcium (figure 16). In the absence of calcium, actin did not bind to gelsolin and thus no fluorescence enhancement was observed. The calcium dependency for actin binding is consistent with work conducted on gelsolin in other laboratories.[42] At an actin to FITC-labelled gelsolin ratio near two, signs of saturation become evident. Since native gelsolin exposes only two actin binding sites, addition of actin beyond a 1:2 stoichiometry is not expected to have pronounced effects on the emission intensities. The gradual intensity increase beyond saturation of the primary binding sites may be attributable to secondary effects that arise from formation of gelsolin capped oligomers of F-actin.

Figure 17 illustrates the change in fluorescence polarization at 520 nm for FITC-labelled gelsolin on titration with actin. Each plot required two sets of samples containing 0.5 μM FITC-labelled gelsolin in 150 mM KCl, 25 mM Tris- HCl, pH 8.0 and either 1 mM EDTA or 1 mM $CaCl_2$. In part a, the titration in the presence of EDTA, no polarization increases were observed

with either the addition of dialysis buffer or actin. In part b, an experiment identical to part a but conducted in the presence of calcium, polarization increases were recorded only upon the addition of actin. These polarization enhancements are likely the result of an increase in size, and thus, the rotational correlation time for the actin-gelsolin protein complex to which FITC is attached. Evidence for calcium specific actin binding is further supported by these observations.

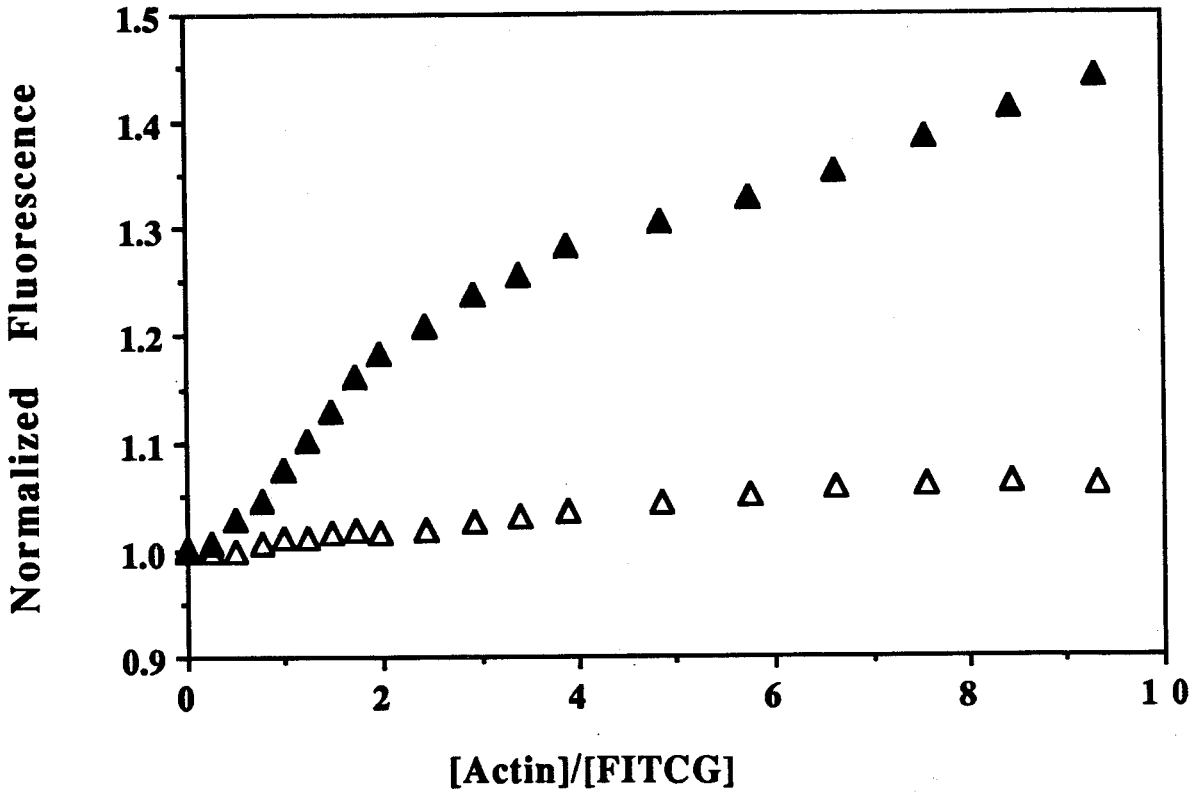

Figure 16 : Fluorescence changes of FITC-labelled gelsolin following the addition of actin. Actin in buffer A was added to a pair of solutions of 0.5 μM FITC-labelled gelsolin in 150 mM KCl, 25 mM Tris-HCl, and either 1 mM EDTA (Δ) or 1 mM $CaCl_2$ (▲), pH 8.0, at 25°C. The excitation wavelength was at 490 nm and the emission wavelength at 520 nm. Normalization was achieved by dividing all the readings by the appropriate sample fluorescence in the absence of actin.

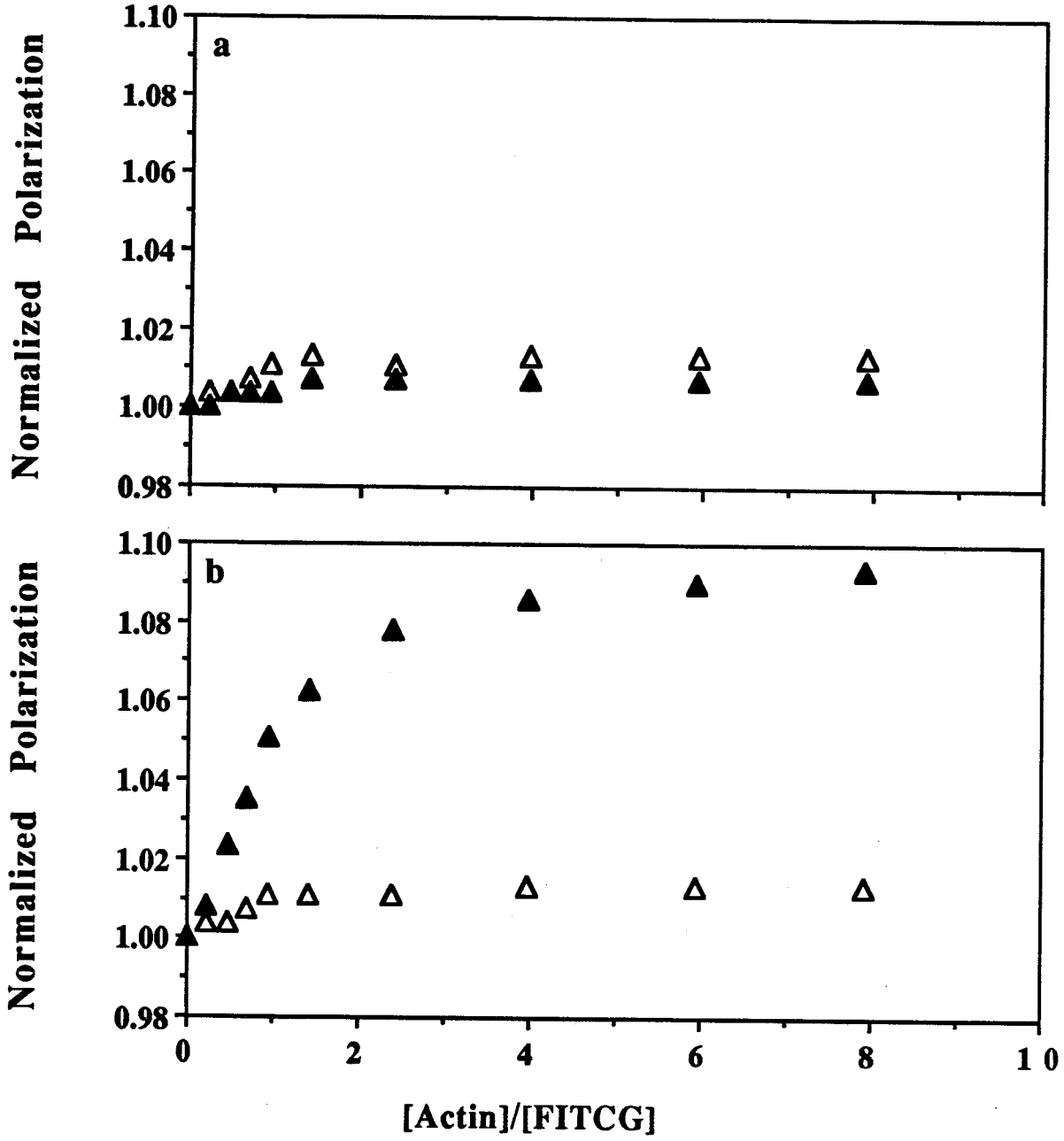

Figure 17 : Fluorescence polarization of FITC-labelled gelsolin following the addition of monomeric actin. (a) Aliquots of actin (▲) and aliquots of buffer A (△) were added to 0.5 μM FITC-labelled gelsolin in 150 mM KCl, 25 mM Tris-HCl, and 1 mM EDTA, pH 8.0, at 25°C. (b) A pair of identical 0.5 μM FITC-labelled samples in 150 mM KCl, 25 mM Tris-HCl, and 1 mM $CaCl_2$, pH 8.0 were titrated with actin (▲) and buffer A (△). Each polarization value was the average of 3 measurements and typical standard deviations were ± 0.002. Excitation was at 490 nm and emission at 520 nm.

1.3 Circular Dichroism Studies

The CD spectrum of FITC-labelled gelsolin in the 240 nm to 205 nm range (figure 18) resembles in shape and intensity the spectra presented by Doi *et al.* for pig plasma gelsolin, and by Reid for native and ACR-labelled horse plasma gelsolin.[75,76] The incorporation of the fluorescein labels did not lead to a change in the overall conformation of gelsolin.

The effects of the fluorescein groups on the gelsolin molecule were further investigated by comparison of the thermal stabilities of both labelled and unlabelled gelsolins. The ellipticity at 215 nm for each protein was recorded at various temperatures until protein denaturation was achieved (figure 19). In the 35°C to 40°C temperature range, FITC-labelled and unlabelled gelsolin in matching solvents behaved similarly, as both proteins passed through a partial unfolding transition. In the unlabelled case, protein stability diminished steadily above 40°C, while gelsolin labelled with FITC proved to be stable up to approximately 55°C. Pronounced loss of 2° structure occurred around the cooperative transition temperatures of approximately 46°C and 58°C for unlabelled and labelled gelsolins, respectively. The enhanced stability of FITC-labelled gelsolin may be attributed to the removal of Lys-NH_2 groups or the introduction of the hydrophobic fluorescein molecules. Above these temperatures both samples lost structure as evident by the appearance of an irreversible precipitate. These results differ significantly from PIA-labelled gelsolin where the

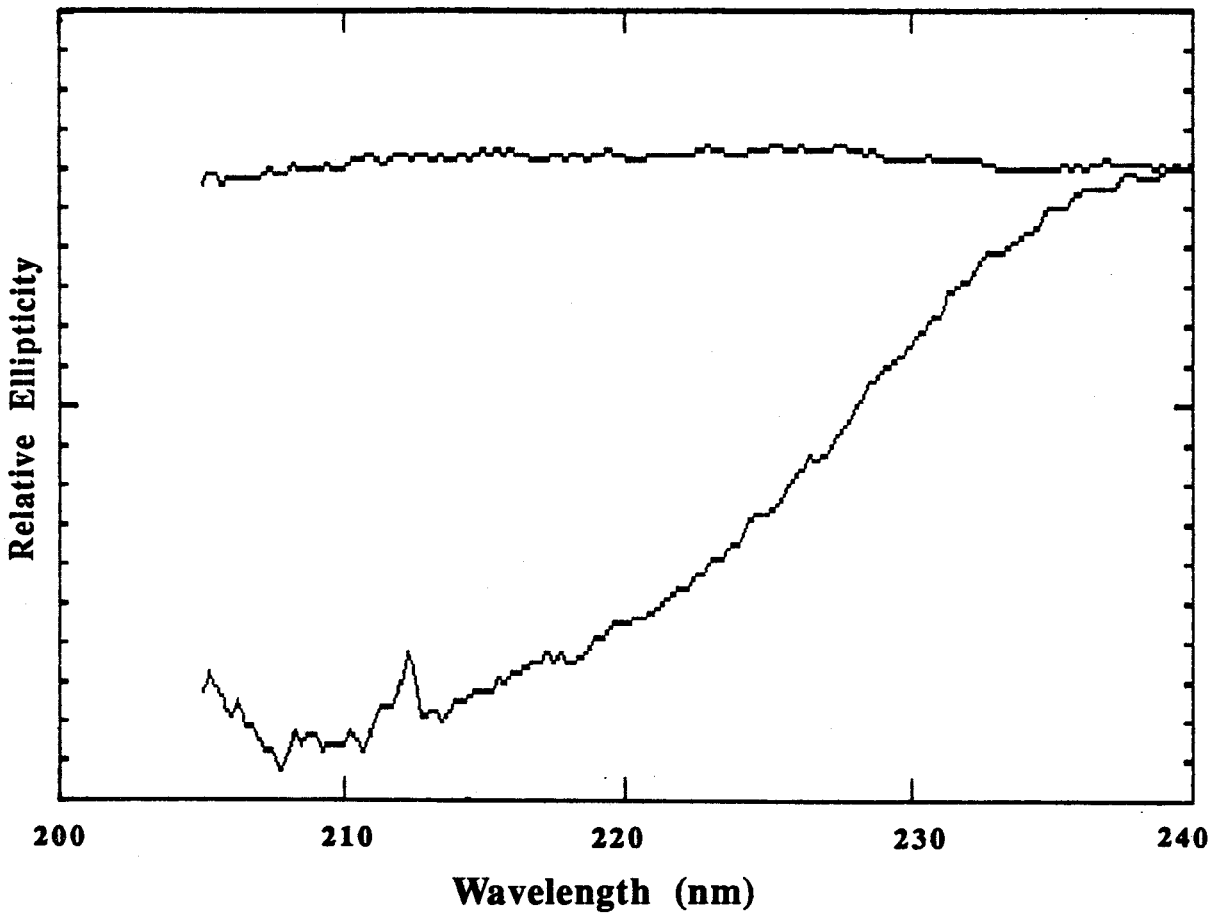

Figure 18 : CD spectrum of FITC-labelled gelsolin. The labelled protein at 0.9 mg/mL was in a solution of 150 mM KCl, 25 mM Tris-HCl, and 1 mM EDTA, pH 8.0, at 25°C. A 0.5 mm pathlength cell was utilised to obtain this spectrum, which is an average of 4 consecutive scans. The baseline is the spectrum of buffer in the absence of protein.

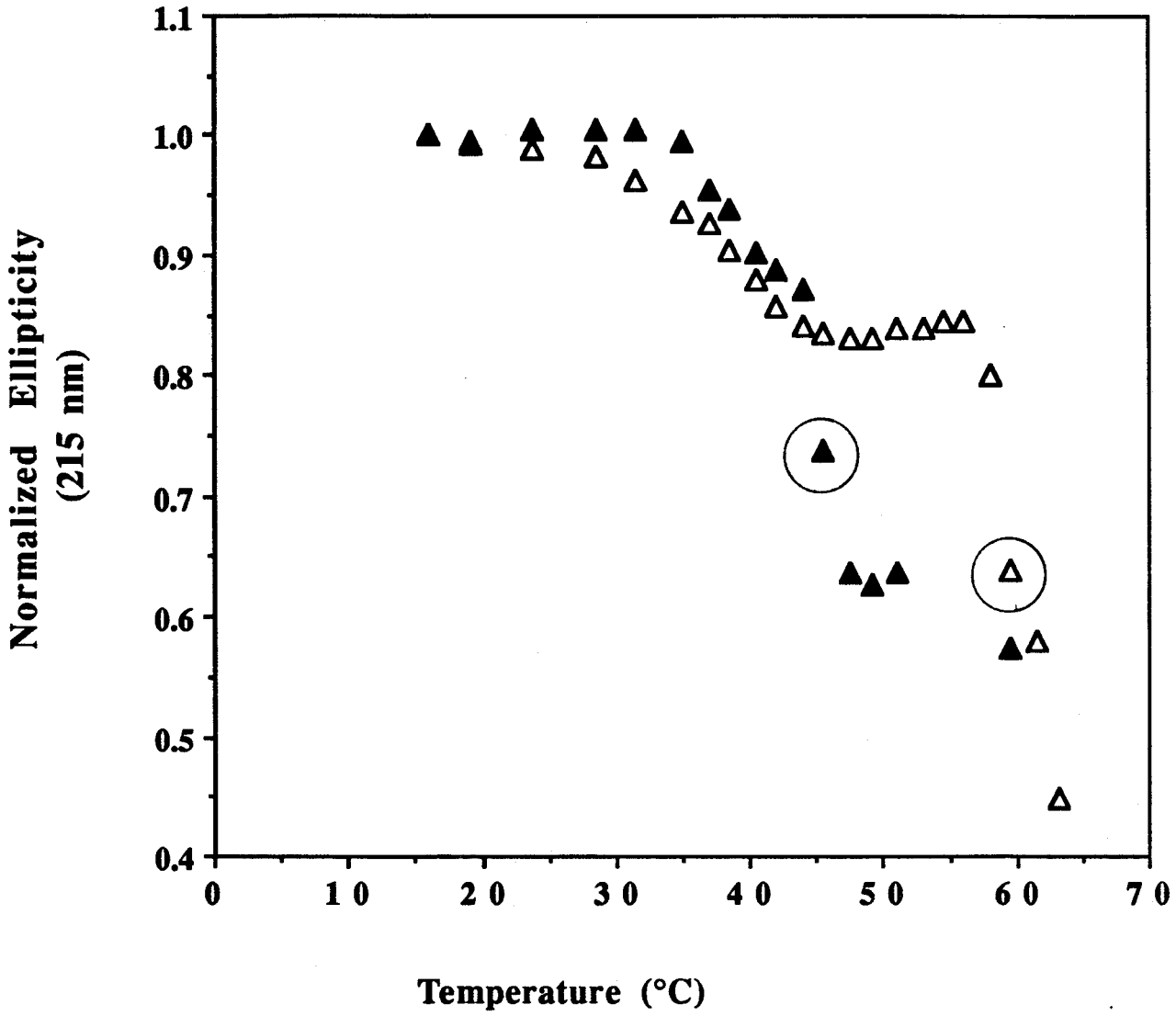

Figure 19 : Changes in normalized ellipticities at 215 nm with temperature of native (▲) and FITC-labelled gelsolin (Δ) in 150 mM KCl, 25 mM Tris-HCl, and 1 mM EDTA, pH 8.0. A 15 minute equilibration period was allowed subsequent to each temperature change. Circled points indicate the onset of precipitation.

labelled protein showed a melting transition 2 to 3°C lower than native gelsolin, and from ACR-labelled gelsolin which revealed identical stabilities for both labelled and unlabelled proteins.[77,76]

Gelsolin conjugated with FITC provided a convenient means of investigating gelsolin structure and monitoring gelsolin-actin interactions. Modification of an average of 5 Lys residues did not alter gelsolin's ability to sever F-actin, but did increase its stability towards thermal denaturation. Upon binding calcium ions, the emission intensity of FITC-labelled gelsolin in low ionic strength buffer increased, supporting the suggestion of an opening up of gelsolin's structure on binding Ca^{+2}.[29] Additional evidence for such a model is provided by the direct titration of FITC-labelled gelsolin with Ca^{+2}, and by fluorescence quenching studies, which showed that quenching by KI is enhanced in the presence of Ca^{+2}.

Upon addition of actin, FITC-labelled gelsolin showed enhanced fluorescence only in the presence of calcium ions. Similarly, fluorescence polarization values of FITC-labelled gelsolin samples titrated with actin increased only in millimolar Ca^{+2}. The fluorescence enhancement observed in both these experiments confirms actin-gelsolin complexation, an event that is regulated by calcium ions.

II. Sulfhydryl Group Modifications

2.1 Gelsolin Modified with Acrylodan

The degree of labelling of gelsolin with acrylodan was 1.1 ± 0.4 (n=5) acrylodans incorporated per gelsolin molecule. When the labelling reaction was carried out in 6 M guanidine-HCl, the degree of labelling increased to 2.8 ± 0.4 (n=3) acrylodans per gelsolin.

Enzymatic cleavage of ACRG with porcine pancreatic α-chymotrypsin also produced a banding pattern that resembles that of human plasma gelsolin.[31,73] By virtue of the two bands found in the 40 to 45 kDa range at very early digestion times, ACRG quickly gets broken down into its NH_2 and COOH terminal domains (figure 20). When observed with a hand held UV lamp prior to staining, bright fluorescence from these two bands was noticed. At longer digestion times, fluorescence of lesser intensity was also detected from lower molecular weight fragments.

The addition of actin to ACR-labelled gelsolin was followed by monitoring emission intensities at 497 nm (figure 21). Two sets of samples were studied, initially containing 1 μM ACRG in 150 mM KCl, 25 mM Tris-HCl, 1 mM DTT, and either 1 mM EDTA or 1 mM $CaCl_2$, pH 8.0, at 25°C. To correct for dilution effects a pair of 1 μM ACRG samples in the above buffers were titrated with buffer A. The fluorescence readings obtained for the actin titration were divided by the buffer readings, and then normalized

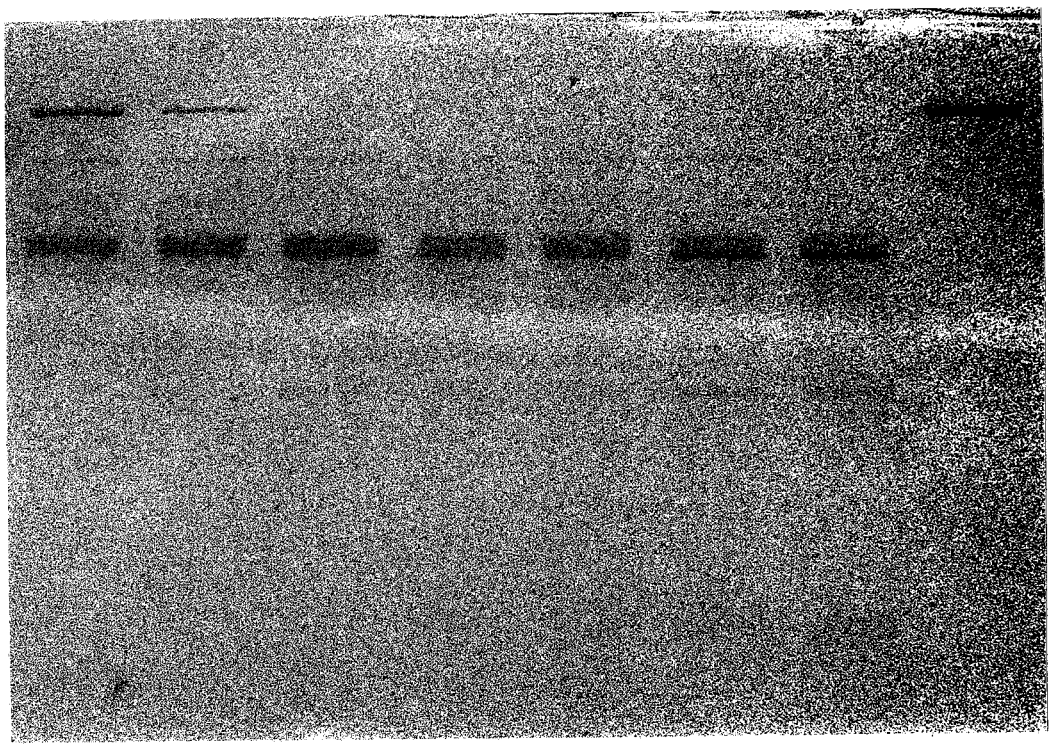

Figure 20 : Limited proteolytic cleavage of ACRG (0.4 mg/mL) with α-chymotrypsin viewed on 12.5% SDS-PAGE gels following Coomassie staining. Starting from the left, the lanes represent the digestion products of 0.5, 1 ,3, 5, 10, 20, and 30 minutes. Undigested horse plasma gelsolin is shown in the lane to the far right.

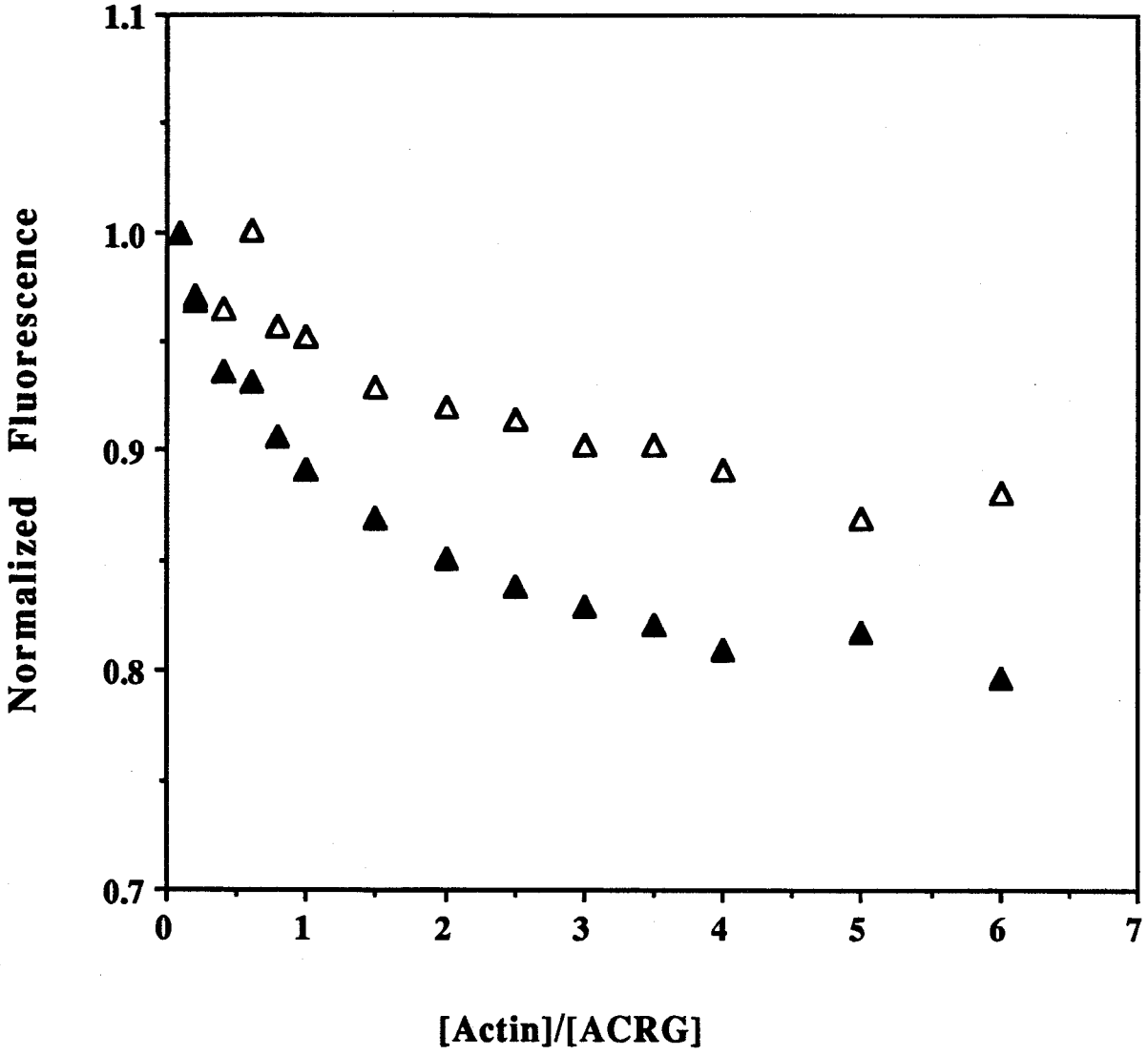

Figure 21 : Titration of ACRG with monomeric actin. One sample initially contained ACRG (1 μM) in 150 mM KCl, 25 mM Tris-HCl, 1 mM DTT, and 1 mM EGTA, pH 8.0, at 25°C (Δ). The other sample was similar but contained 1 mM $CaCl_2$ instead of the EGTA (▲). Excitation was at 390 nm and emission at 497 nm. Corrections for dilution were made according to the text.

accordingly.

A steady drop in emission intensity is evident upon the addition of actin in both EDTA and Ca^{+2} containing buffers, suggesting an interaction between these two proteins that results in acrylodan fluorescence quenching. The effective quenching is more prominent in the presence of calcium, but clearly this cation is not the sole contributing factor to the fluorescence decrease. An increase in exposure of the ACR label to solvent in calcium further supports the suggestion of gelsolin's structure opening upon binding calcium.[29]

To investigate the acrylodan probe environment, the change in fluorescence polarization at 497 nm was monitored for ACRG titrated with actin. Two sets of samples were studied, each initially containing 1 μM ACRG in 150 mM KCl, 25 mM Tris-HCl, 1 mM DTT, and either 1 mM EDTA or 1 mM $CaCl_2$, pH 8.0 (figure 22). Equal volumes of buffer A were added to a couple of otherwise identical samples, serving to control for dilution effects.

Polarization values were observed to increase on the addition of actin only when calcium was present, confirming the calcium requirement for actin binding. For the experiment in EDTA, polarization values at ratios of 1, 2, 3, and 5 were the same for both the actin and buffer A titrations. As was the case with polarization studies done with FITC-labelled gelsolin, complex formation results in a size increase, which in turn increases the rotational correlation time for the actin-ACRG complex to which the fluorophores are attached.

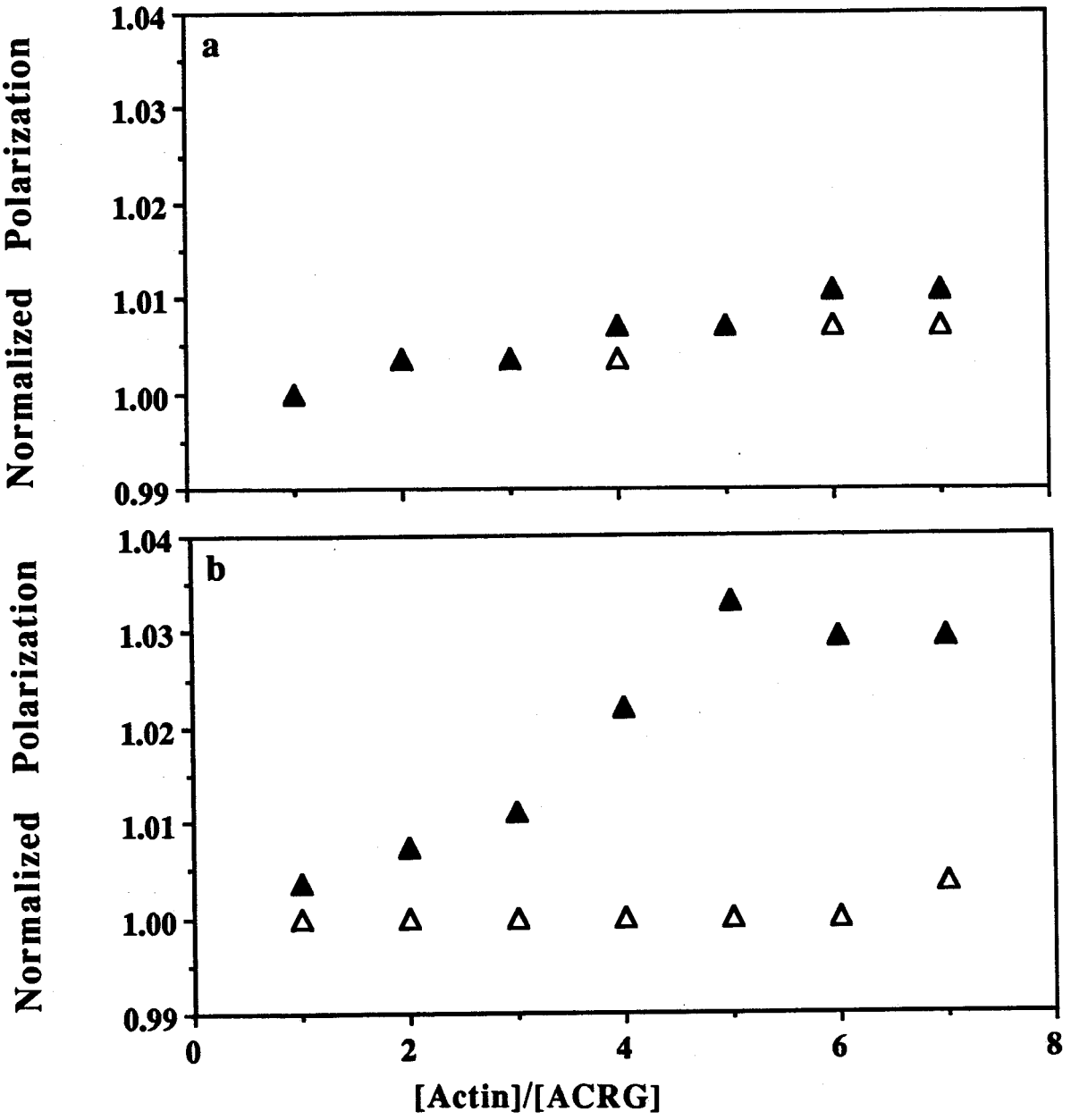

Figure 22 : Fluorescence polarization changes of ACRG following the addition of monomeric actin. (a) Two samples of ACRG (1 μM) in 150 mM KCl, 25 mM Tris-HCl, 1 mM DTT, and 1 mM EGTA, pH 8.0, at 25°C were titrated with aliquots of either actin (▲) or buffer A (Δ). In a similar experiment (b), two samples of ACRG (1 μM) in 150 mM KCl, 25 mM Tris-HCl, 1 mM DTT, and 1 mM $CaCl_2$ were also titrated with actin (▲) or buffer A (Δ). Each polarization value was the average of three measurements with typical standard deviations of ± 0.002. Excitation and emission was at 390 nm and 497 nm, respectively.

2.2 Reaction with DTNB and Derivatisation with Pyrene

The average number of gelsolin thiol groups available for reaction with 5,5'-dithiobis(2-nitrobenzoic acid) or DTNB (Ellman's reagent) was found to be 1.1 ± 0.3 based on three separate trials. When this reaction was carried out in 6 M guanidine-HCl, 3.3 ± 0.3 (n=3) thiol groups were found to be accessible to Ellman's reagent. The assay was conducted using three different thiol containing compounds, 2-mercaptoethanol, dithiothreitol, and glutathione to prepare standard curves, all of which yielded similar results.

A further investigation of gelsolin thiol content was undertaken using N-(1-pyrene)iodoacetamide (PIA). Extensive work conducted in this laboratory by Ruiz Silva with PIA-labelled gelsolin has shown that under non-denaturing conditions 1.6 ± 0.3 pyrenes could be incorporated per gelsolin.[77] Upon repeating the labelling reaction in 6 M guanidine-HCl during the course of the present work, the degree of labelling increased to 4.1 ± 0.4, a value determined by three separate trials.

As evident by these modification results (Table 2), not all thiol groups on gelsolin are exposed to reagent when the protein is in the native state. Additionally, only 3 to 4 thiols groups were detectable, a lower total than the 5 reported for human and pig plasma gelsolins.[23,25] Ultimately, the thiol content will have to be determined by a complete amino acid analysis, or by protein sequencing. The discrepancy between the DTNB and the PIA results may be due to, in part, an error in the published absorption coefficient. The

literature value employed was derived from the pyrenyl-actin complex and could deviate somewhat from the value for PIA-labelled gelsolin.

Table 2 : Summary of Gelsolin Thiol Modifications

	Labelling Conditions	
Reagent	**Native**	**Denatured**
ACRG	1.1 ± 0.4	2.8 ± 0.4
DTNB	1.1 ± 0.3	3.3 ± 0.1
PIA	1.6 ± 0.3	4.1 ± 0.4

The effectiveness of the 6 M guanidine-HCl chemical denaturation was examined by fluorescence spectra taken immediately after S-alkylation with PIA (figure 23). Upon excitation at 340 nm, two monomer emission peaks at 385 nm and 407 nm are observable. Noticeably missing is the large broadband excimer emission peak centred around 480 nm. Loss of 2° structure diminishes stacking of two PIA-derivatised Cys residues that are otherwise in close proximity to one another. Extensive dialysis of this sample against 150 mM KCl, 25 mM Tris-HCl, 1 mM EGTA, pH 8.0, at 4°C removed the guanidine-HCl. The emission spectrum of this partially refolded sample shows strong excimer fluorescence, with an excimer to 385 nm monomer emission ratio of approximately 2.4 (figure 24). In comparison, PIA-labelled gelsolin in its native state yields an excimer to monomer ratio of

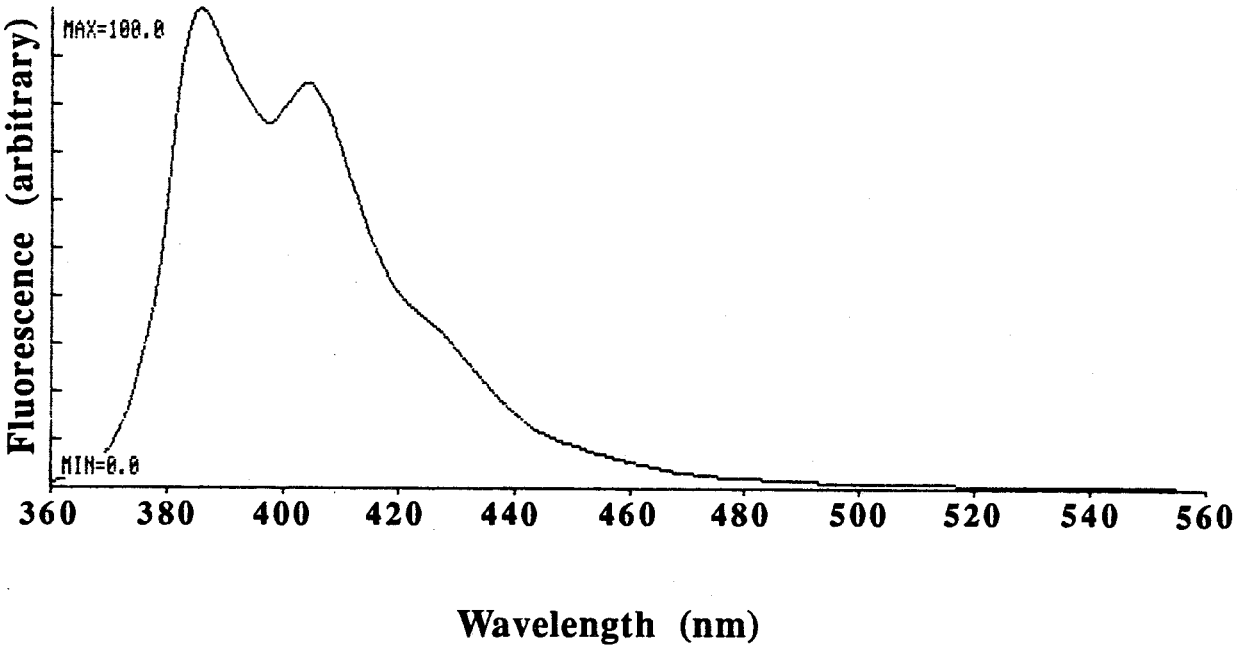

Figure 23 : Emission spectrum of PIA-modified gelsolin that was labelled in denaturing conditions. The protein was in 150 mM KCl, 25 mM Tris-HCl, 1 mM EGTA, pH 8.0 and made up to 6 M guanidine-HCl at 25°C. The excitation wavelength was set at 340 nm.

a

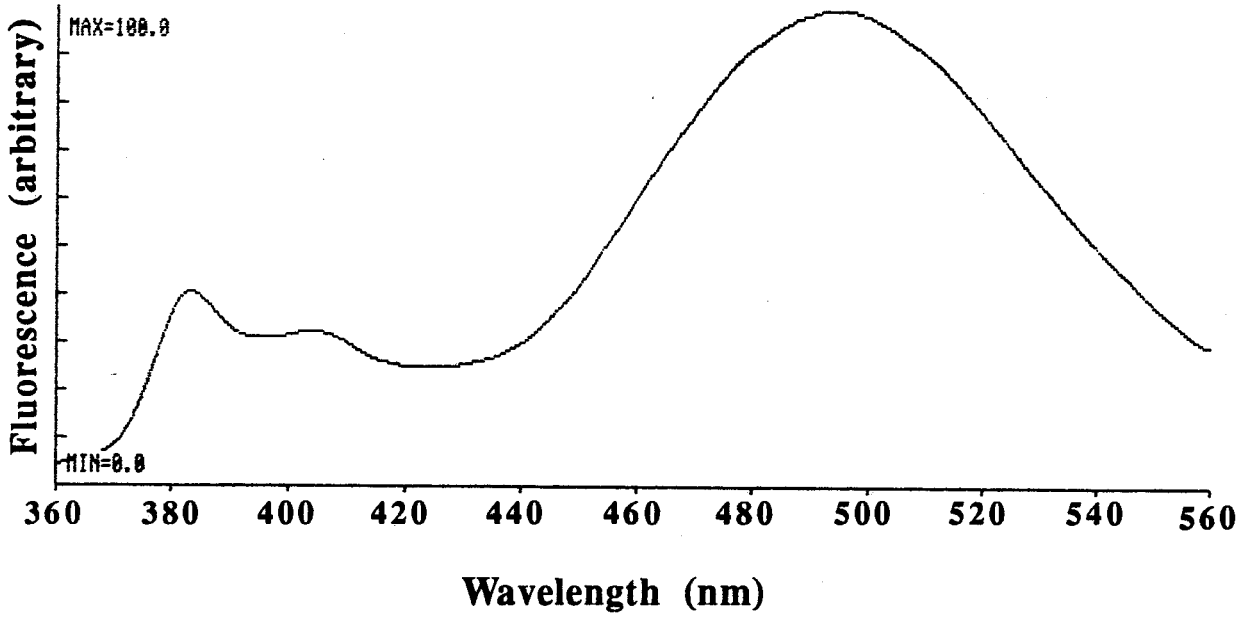

b

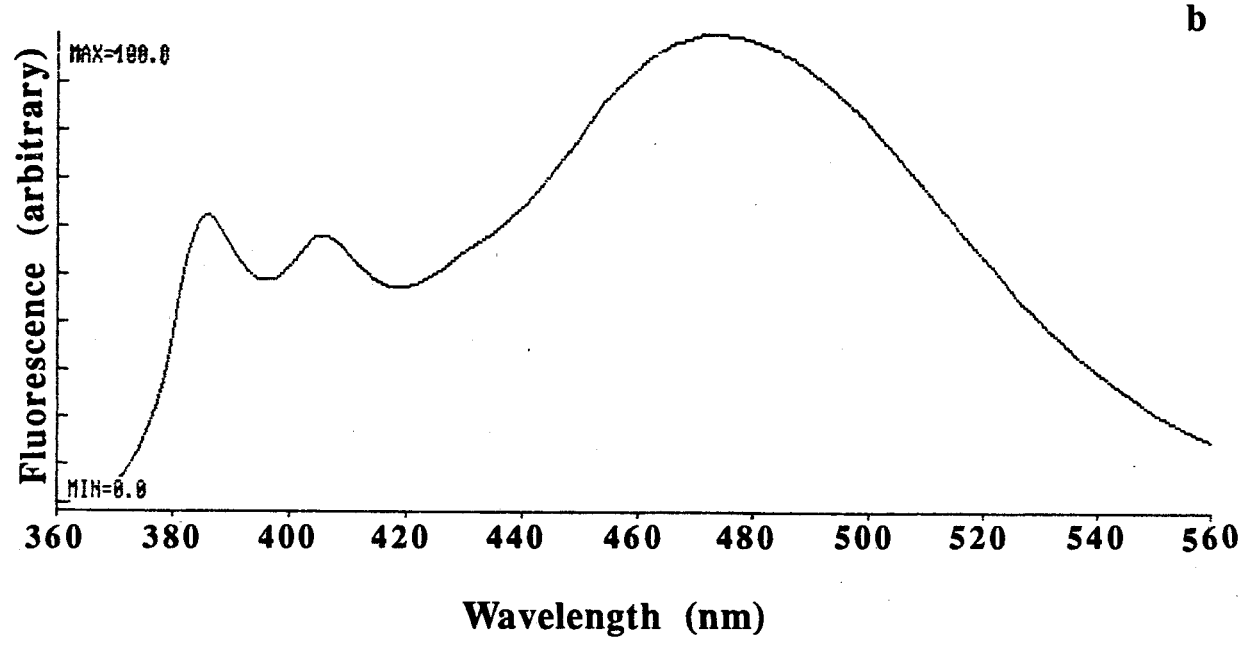

Figure 24 : (a) Fluorescence spectrum of pyrene-gelsolin that was labelled in denaturing conditions and subsequently renatured. Solution conditions were 150 mM KCl, 25 mM Tris-HCl, and 1 mM EGTA, pH 8.0. (b) Addition of 6 M guanidine-HCl to the sample from (a). The excitation wavelength for both spectra was set at 340 nm.

approximately 4.[77] Interestingly, attempts to denature this sample a second time appeared not to work. The addition of guanidine-HCl to a concentration of 6 M did not abolish the excimer fluorescence, even at elevated temperatures. These observations suggest that denatured gelsolin does not refold to its native conformation.

Sulfhydryl modifications with the thiol specific reagents ACR, PIA, and DTNB showed that in its native state, gelsolin exposes between 1 and 2 cysteine groups. Under denaturing conditions, approximately 3 thiol groups could be labelled. Once denatured, the F-actin severing activity of gelsolin could not be fully restored upon renaturation. Only a 7% reduction in viscosity of F-actin could be achieved at a mole ratio of ACR-gelsolin to actin of 1 : 50.

Actin binding studies with ACR-gelsolin support results obtained with FITC-labelled gelsolin. For actin-gelsolin complexation, Ca^{+2} must be present. Upon binding actin or calcium, exposure of the acrylodans to solvent resulted in fluorescence quenching, while a fluorescence enhancement was obtained with the FITC chromophores. Both of these observations are consistent with greater exposure of the fluorophores to solvent.

III. Gelsolin Interactions with Tropomyosin

3.1 Fluorescence Titration and C-TM Affinity Chromatography

Aliquots of skeletal tropomyosin (S-TM) in 150 mM KCl, 25 mM Tris-HCl, and 1 mM EDTA, pH 8.0 were added to a 0.25 μM FITC-labelled gelsolin solution at 25°C (Figure 25). The open triangles represent data collected on addition of stock S-TM in EDTA, while the closed triangles were for an identical experiment but the EDTA was substituted with 1 mM $CaCl_2$. To correct for dilution, the fluorescence intensity of each sample was divided by the fluorescence intensity of an identical sample to which buffer was added instead of S-TM. A fluorescence enhancement was observable only in the presence of calcium ions, indicating that the gelsolin-tropomyosin interaction is calcium sensitive. Quantitative analysis of this data according to a method by Bagshaw and Harris yields two independent tropomyosin binding sites on gelsolin, each with a dissociation constant of approximately 0.6 μM.[78]

Further support for a calcium specific gelsolin-tropomyosin interaction was provided by a tropomyosin-agarose affinity matrix. In the presence of Ca^{+2}, FITC-labelled gelsolin was retained on the affinity column, but in its absence no binding was observed. Protein elution was achieved by the application of a linear 0 to 500 mM KCl gradient made up in equilibration

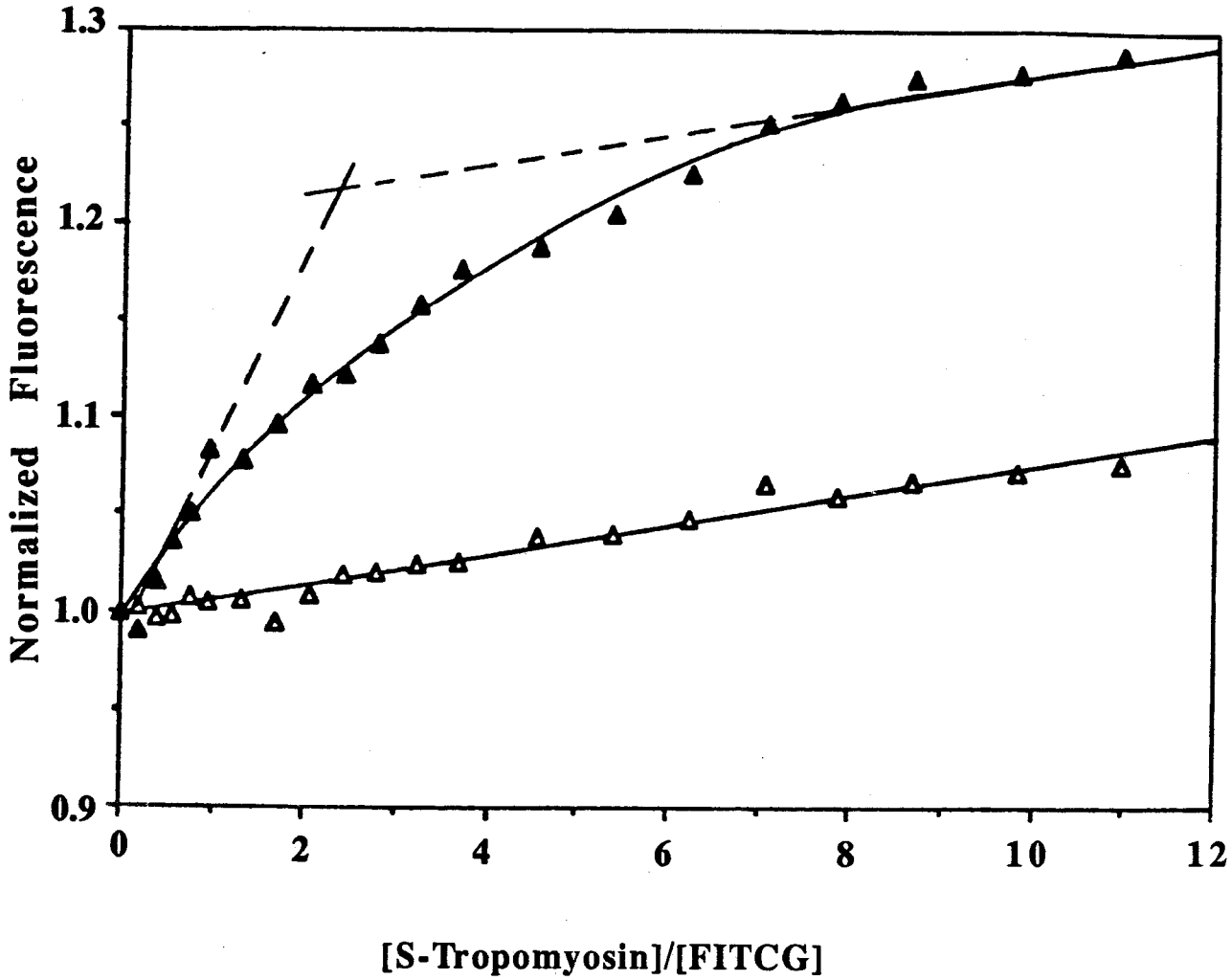

Figure 25 : Titration of FITC-labelled gelsolin with skeletal tropomyosin. Stock S-TM in 150 mM KCl, 25 mM Tris-HCl, and either 1 mM EDTA (Δ) or 1 mM $CaCl_2$ (▲), pH 8.0, was added to 0.25 μM FITC-gelsolin in the same buffer. To a pair of identical samples, equal volumes of buffer were added. Corrections for dilutions were made by dividing the fluorescence intensity of each sample by the buffer readings. Titrations were performed at 25°C, with 490 nm excitation and 520 nm emission wavelengths.

buffer (Figure 26). SDS-polyacrylamide gel electrophoresis confirmed that the eluted protein was indeed gelsolin. A single fluorescent band was observable at a position that matched that of unlabelled gelsolin after staining. Since these results were reproducible with gelsolin modified by acrylodan, the gelsolin-tropomyosin interactions are not likely to be a result of the covalently bound fluorophores. The retention of gelsolin at ionic strengths up to approximately physiological levels may reflect a possible biological function.

An investigation of gelsolin's actin-severing activity in the presence of tropomyosin has been carried out by Ishikawa *et al.*, who found that the severing activity of gelsolin on actin is diminished by tropomyosin.[79] This observation was explained by assuming that tropomyosin and gelsolin compete in actin binding, while sharing the same binding site on an actin molecule. Results from the present study suggests that gelsolin interacts with tropomyosin directly, and that the interaction is Ca^{+2} sensitive. Perhaps it is the direct interaction between gelsolin and tropomyosin that decreases gelsolin's F-actin severing activity in the ternary actin-gelsolin-tropomyosin complex.

3.2 Photochemical Crosslinking

Gelsolin labelled with benzophenone-4-isothiocyanate (BITC) was added to a solution of cardiac tropomyosin (C-TM) and irradiated up to 60

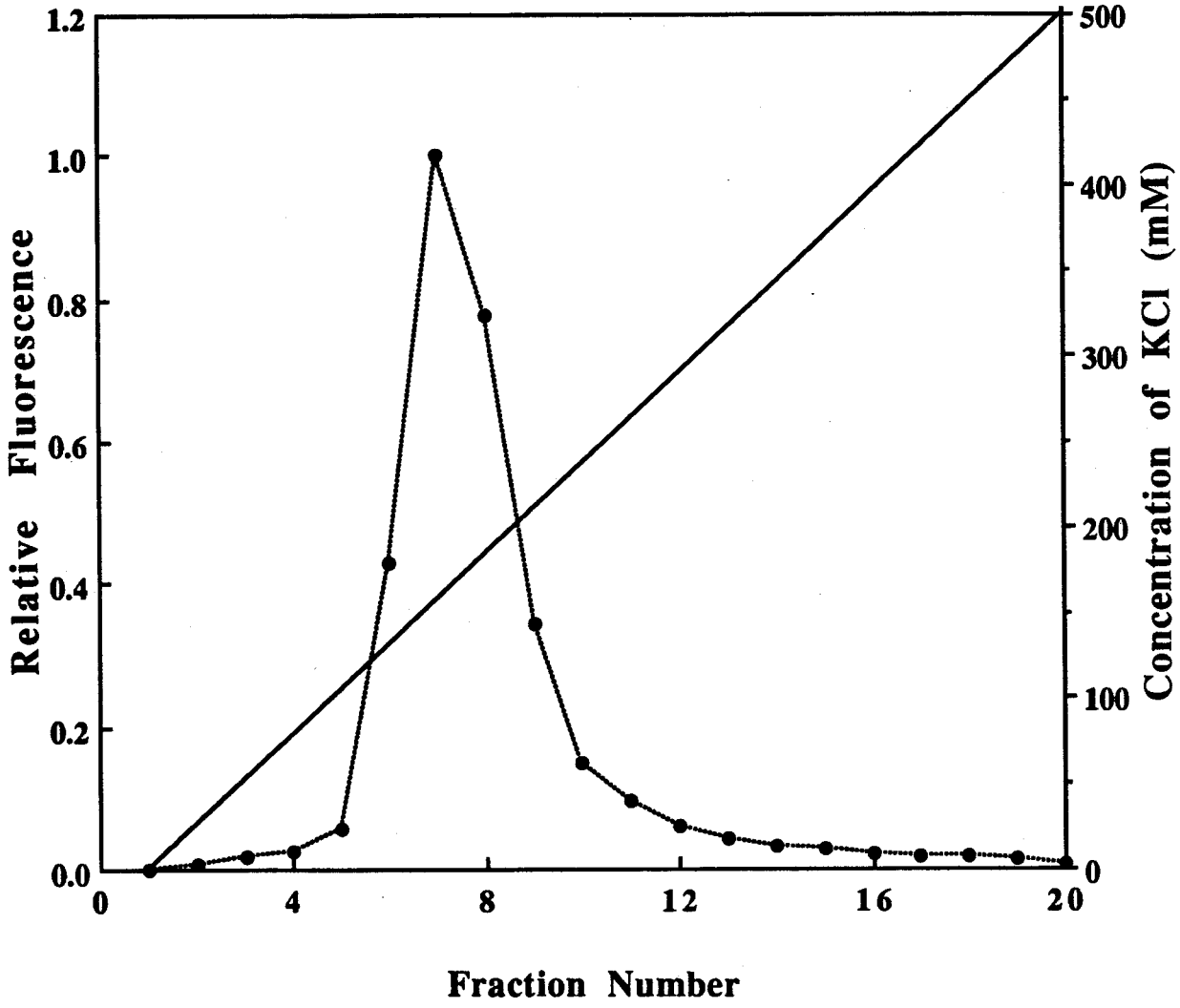

Figure 26 : Skeletal tropomyosin affinity chromatography. FITC-labelled gelsolin was loaded onto a TM-agarose column that was equilibrated with 25 mM Tris-HCl, and 1 mM $CaCl_2$, pH 8.0. After extensive washing with equilibration buffer, a 0 to 500 mM KCl gradient in equilibration buffer was applied and 2 mL fractions collected. An excitation wavelength of 490 nm and an emission wavelength of 520 nm was used to monitor the eluant.

minutes. The appearance of high molecular weight bands on SDS-polyacrylamide gels confirm that gelsolin forms a complex with tropomyosin in calcium containing buffers (figure 27). Photoactivation of BITC-labelled gelsolin in the absence of C-TM did not reveal any crosslinked products, ruling out photo induced intermolecular gelsolin polymerization. When the irradiation was conducted in EDTA buffer, only trace amounts of crosslinked products were detected (data not shown).

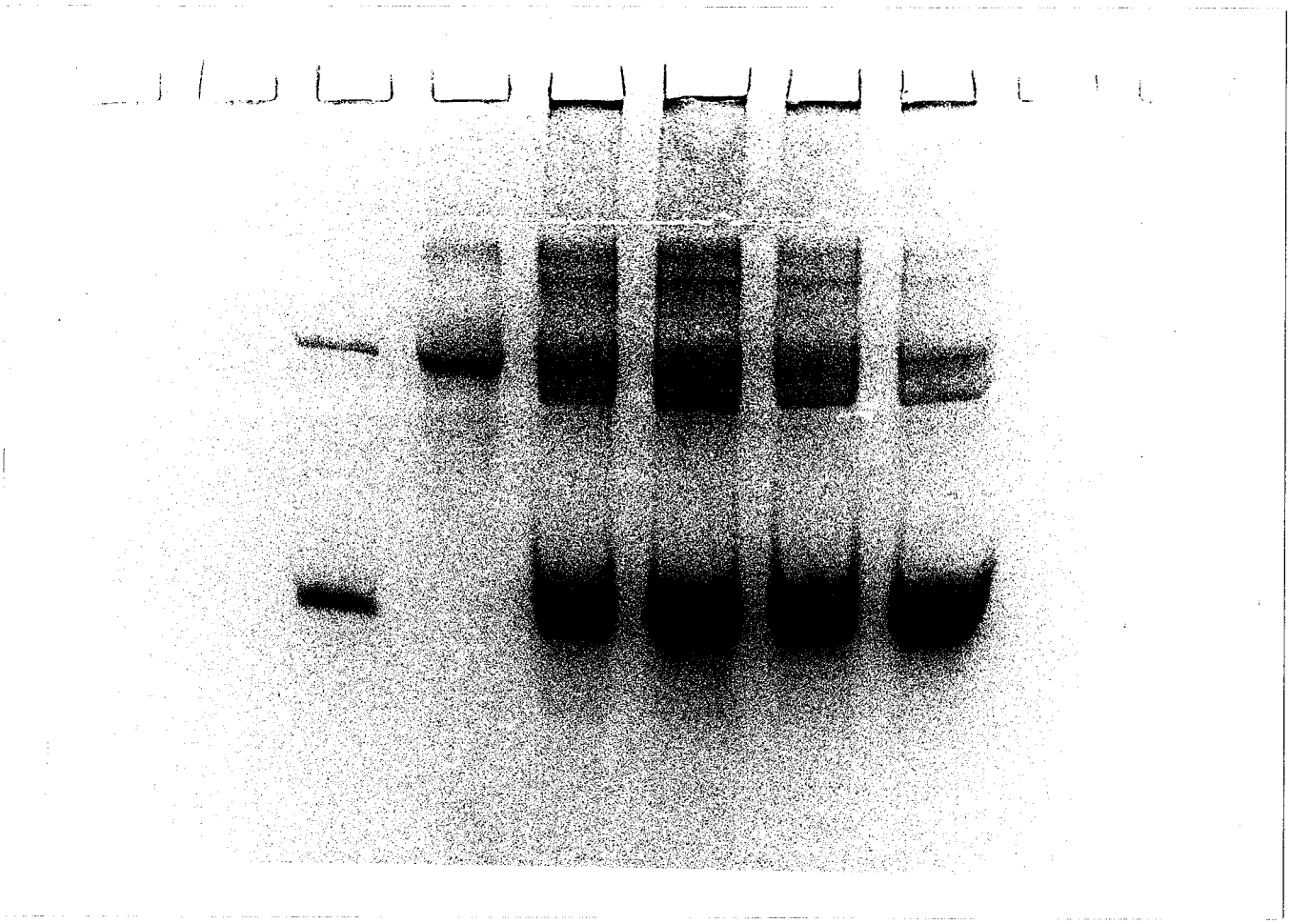

Figure 27 : Photochemical crosslinking of a solution containing a 10 : 1 mole ratio of C-TM to BITC-labelled gelsolin prepared in 25 mM Tris-HCl, 1 mM EDTA, pH 8.0 and made up to 2 mM $CaCl_2$ The sample, in a 4°C water-cooled, 1 cm quartz cuvet was irradiated with a 200 W Hg arc lamp. Starting from the right, lanes 1 through 4 are aliquots of the irradiated sample at 15, 30, 45, and 60 minutes. The lane on the extreme left contains unlabelled gelsolin and C-TM, while the second lane from the left demonstrates BITC-labelled gelsolin irradiated alone for 60 minutes.

IV. Conclusion

4.1 Summary of Results

Fluorescence studies with the covalent probe fluorescein-5-isothiocyanate indicated that up to six Lys residues of gelsolin can be labelled. When FITC-labelled gelsolin was added to F-actin, solution viscosities decreased in an amount dependent on the gelsolin concentration. At an actin to FITC-labelled gelsolin mole ratio of 50:1, labelled gelsolin exhibited full activity with respect to F-actin severing. Limited cleavage of FITC-gelsolin by α-chymotrypsin indicates incorporation of the fluorophores at various sites along the peptide sequence.

Upon binding Ca^{+2}, the emission intensity of FITC-gelsolin in low ionic strength buffer increased by 25%. In high ionic strength solutions, Debye screening masks the Ca^{+2} binding sites. The increase in fluorescence may be the result of an increased exposure of the fluorescein moieties to polar solvent. This, along with the greater degree of fluorescence quenching observed in the presence of Ca^{+2}, supports the suggestion of an opening of gelsolin's structure upon binding calcium.[29]

Investigations of actin binding to gelsolin were carried out with FITC- and ACR-labelled gelsolins. The fluorescence of FITC-gelsolin increased on addition of actin in a Ca^{+2} dependent manner. Fluorescence titration studies of ACR-gelsolin also revealed actin binding, but with this probe, a decrease in the

fluorescence intensity was recorded. These two observations suggest that on binding actin, there is an increased exposure of some of the fluorophores to solvent. Actin-gelsolin complexation was confirmed by fluorescence polarization experiments, which showed that polarization values increased on addition of actin to both FITC- and ACR-labelled gelsolins in calcium containing buffers.

The success of monitoring actin-gelsolin interactions with FITC-labelled gelsolin prompted an investigation of novel gelsolin interactions with tropomyosin.[80] Studies undertaken in this thesis show for the first time that tropomyosin binds to plasma gelsolin in a Ca^{+2} specific manner. This observation is supported by retention of labelled gelsolins on a tropomyosin-agarose affinity column, and from a fluorescence enhancement of FITC-gelsolin on addition of actin. Additionally, solutions of benzophenone-4-isothiocyanate labelled gelsolin with tropomyosin revealed high molecular weight bands on SDS-PAGE upon photoactivation, indicating an intermolecular interaction between these two proteins.

4.2 Suggestion for Further Study

Covalent modification with FITC creates a probe which may be used to monitor the binding of Ca^{+2}, actin and tropomyosin to horse plasma gelsolin. Modifications of Lys residues on pig plasma gelsolin with 4-fluoro-7-nitrobenz-2-oxa-1,3 diazole showed one slowly reacting Lys group which was essential for

binding to actin.[81] Under the FITC labelling reaction conditions employed in the present study, a Lys group essential for actin binding was not derivatised. Attempts to locate this slowly reacting Lys group by modification of the present FITC labelling reaction conditions may give additional insight to gelsolin-actin interactions. A further investigation of the labels in FITC-gelsolin may require determining their locations in the protein sequence by standard peptide sequence analysis. In addition to locating the fluorescent labels, this work would also provide the 1° structure for horse plasma gelsolin, which could then be used to accurately assess the number of cysteine groups in the molecule. Comparison of the horse plasma sequence with those for human and pig plasma gelsolins would give an indication of gelsolin homology between different species.

Perhaps the most interesting direction for additional studies would involve a comprehensive analysis of gelsolin-tropomyosin interactions. This would initially include a complete characterisation of the gelsolin-tropomyosin association, followed by investigations of the ternary actin-gelsolin-tropomyosin protein system. Eventually, investigations of gelsolin-tropomyosin interactions should reveal if these association have any biological ramifications.

References

1. Straub, F.B. (1942) *Studies University of Szeged* **2**, 3-15

2. Mommaerts, W.F. (1992) *Bioessays* **14**, 57-59

3. Korn, E.D. (1982) *Physiol. Rev.* **62**, 672-737

4. Weeds, A. (1982) *Nature* **296**, 811-816

5. Stossel, T.P., Chaponnier, C., Ezzell, R.M., Hartwig, J.H., Janmey, P.A., Kwiatkowski, D.J., Lind, S.E., Smith, D.B., Southwick, F.S., Yin, H.L., and Zaner, K.S. (1985) *Ann. Rev. Cell Biol.* **1**, 353-402

6. Carlier, M.-F. (1991) *J. Biol. Chem.* **266**, 1-4

7. Holmes, K.C., Popp, D., Gebhard, W., and Kabsch, W. (1990) *Nature* **347**, 44-49

8. Stryer, L. (1981) "Biochemistry" Second Edition, W. H. Freeman and Company, New York

9. Pollard, T.D., and Cooper, J.A. (1986) *Ann. Rev. Biochem.* **55**, 987-1035

10. Kabsch, W., Mannherz, H.G., Suck, D., Pai, E.F., and Holmes, K.C. (1990) *Nature* **347**, 37-44

11. Craig, S.W., and Pollard, T.D. (1982) *Trends Biochem. Sci.* **46**, 88-92

12. Way, M., and Weeds, A. (1990) *Nature* **344**, 292-294

13. Smillie, L.B. (1979) *Trends Biochem. Sci.* **43**, 151-155

14. Côté G.P. (1983) *Mol. Cell. Biochem.* **57**, 127-146

15. Yin, H.L., and Stossel, T.P. (1979) *Nature* **281**, 583-586

16. Yin, H.L., Zaner, K.S., and Stossel, T.P. (1980) *J. Biol. Chem.* **255**, 9494-9500

17. Yin, H.L., Albrecht, J.H., and Fattoum, A. (1981) J. *Cell Biol.* **91**, 901-906

18. Yin. H.L., Kwiatkowski, D.J., Mole, J.E., and Cole, F.S. (1984) *J. Biol. Chem.* **259**, 5271-5276

19. Nodes, B.R., Shackelford, J.E., and Lebherz, H.G. (1987) *J. Biol. Chem.* **262**, 5422-5427

20. Kwiatkowski, D.J., Mehl, R., Izumo, S., Nadal-Ginard, B., and Yin, H.L. (1988) *J. Biol. Chem.* **263**, 8239-8243

21. Harris, H.E., Bamburg, J.R., and Weeds, A.G. (1980) *FEBS Lett.* **121**, 175-182

22. Harris, H.E., and Gooch, J. (1981) *FEBS Lett.* **123**, 49-53

23. Kwiatkowski, D.J., Stossel, T P., Orkin, S.H., Mole, J.E., Colten, H.R., and Yin, H.L. (1986) *Nature* **323**, 455-458

24. Kwiatkowski, D J., Mehl, R., and Yin, H.L. (1988) *J. Cell Biol.* **106**, 375-384

25. Way, M., and Weeds, A. (1988) *J. Mol. Biol.* **203**, 1127-1133

26. Wickner, W.T., and Lodish, H. (1985) *Science* **230**, 400-407

27. Tellam, R.L. (1991) *Arch. Biochem. Biophys.* **288**, 185-191

28. Bryan, J. (1988) *J. Cell Biol.* **106**, 1553-1562

29. Way, M., Gooch, J., Pope, B., and Weeds, A.G. (1989) *J. Cell. Biol.* **109**, 593-605

30. Kwiatkowski, D.J., Janmey, P.A., and Yin, H.L. (1989) *J. Cell Biol.* **108**, 1717-1726

31. Bryan, J., and Hwo, S. (1986) *J. Cell Biol.* **102**, 1439-1446

32. Hwo, S., and Bryan J. (1986) *J. Cell Biol.* **102**, 227-236

33. Bryan, J., and Kurth, M. (1984) *J. Biol. Chem.* **259**, 7480-7487

34. Janmey, P.A., Chaponnier, C., Lind, S.E., Zaner, K.S., Stossel, T.P., and Yin, H.L. (1985) *Biochemistry* **24**, 3714-3723

35. Harris, H.E., and Weeds, A.G. (1983) *Biochemistry* **22**, 2728-2740

36. Pope, B., Way, M., and Weeds, A G. (1991) *FEBS Lett.* **280**, 70-74

37. Bearer, E.L. (1991) *J. Cell Biol.* **115**, 1629-1683

38. Harris, H.E., and Weeds, A.G. (1984) *FEBS Lett.* **177**, 184-188

39. Janmey, P.A., and Stossel, T.P. (1987) *Nature* **325**, 362-364

40. Janmey, P.A., Iida, K., Yin, H.L., and Stossel, T.P. (1987) *J. Biol. Chem.* **262**, 12228-12236

41. Lassing, I., and Lindberg, U. (1985) *Nature* **314**, 472-474

42. Yin., H.L. (1987) *BioEssays* **7**, 176-179

43. Cunningham, C.C., Stossel, T.P., and Kwiatkowski, D.J. (1991) *Science* **251**, 1233-1236

44. Ito, H., Kambe, H., Kimura, Y., Nakamura, H., Hayashi, E., Kishimoto, T., Kishimoto, S., and Yamamoto, H. (1992) *Gastroenterology* **102**, 1668-1692

45. Lind, S.E., Smith, D.B., Janmey, P.A., and Stossel, T.P. (1988) *Am. Rev. Respir. Dis.* **138**, 429-434

46. Lees, A., Haddad, J.G., and Lin, S. (1984) *Biochemistry* **23**, 3038-3047

47. Coué, M., Constants, J., and Olomucki, A. (1986) *Eur. J. Biochem.* **160**, 273-277

48. Lind, S.E., Smith, D.B., Janmey, P.A., and Stossel, T.P. (1986) *J. Clin. Invest.* **78**, 736-742

49. Szabo, A.G. (1989) "The Enzyme Catalysis Process", Plenum Publishing Corporation

50. Schulman, S.G. (1977) "Fluorescence and Phosphorescence Spectroscopy: Physiochemical Principles and Practice" , Pergamon Press, Toronto

51. Freed, K.F. (1978) *Acc. Chem. Res.* **11**, 74-80

52. Lowry, T.H., and Richardson, K.S. (1987) "Mechanism and Theory in Organic Chemistry" Third Edition, Harper & Row Publishers, New York

53. Harris, D.C. (1987) "Quantitative Chemical Analysis" Second Edition, W. H. Freeman and Company, New York

54. Lakowiz, J.R. (1984) "Principles of Fluorescence Spectroscopy", Plenum Press, New York

55. Kasha, M. (1952) *J. Chem. Phys.* **20**, 71-74

56. Cantor, C.R., and Schimmel, P.R. (1980) "Biophysical Chemistry Part II", W. H. Freeman and Company, San Francisco

57. Freifelder, D. (1976) "Physical Biochemistry", W.H. Freeman and Company, San Franscisco

58. Argos, P., and MohanaRao, J.K. (1986) *Methods Enzymol.* **130**, 185-256

59. Greenfield, N., and Fasman, D. (1969) *Biochem.* **8**, 4108-4116

60. Saxena, V.P., and Wetlaufer, B.D. (1971) *Proc. Natl. Acad. Sci.*, USA **68**, 969-972

61. Spudich, J.A., and Watt, S. (1971) *J. Biol. Chem.* **246**, 4866-4871

62. Gordon, D.J., Yang, Y.-Z., and Korn, E.D. (1976) *J. Biol. Chem.* **251**, 7474-7479

63. Laemmli, U.K. (1970) *Nature* **227**, 680-685

64. Ito, H., Yamamoto, H., Yoshihiro, K., Kambe, H., Okochi, T., and Kishimoto, S. (1990) *J. Chromatog.* **526**, 397-406

65. Ruiz Silva, B.E., and Burtnick, L.D. (1990) *Biochem. Cell Biol.* **68**, 796-800

66. Smillie, L.B. (1982) *Methods Enzymol.* **85**, 234-241

67. Burtnick, L.D. (1984) *Biochim. et Biophys. Acta* **791**, 57-62

68. Bradford, M. (1976) *Anal. Biochem.* **72**, 248-254

69. Bernhardt, R., Dao, N., Stiel, H., Schwarze, W., Friedrich J., Jänig, G.-R., and Ruckpaul, K. (1983) *Biochim. et Biophys. Acta* **745**, 140-148

70. Prendergast, F.G., Meyer, M., Carlson, G.L., Iida, S., and Potter, J.D. (1983) *J. Biol. Chem.* **258**, 7541-7544

71. Kouyama, T., and Mihashi, K. (1981) *Eur. J. Biochem.* **114**, 33-38

72. Riddles, P.W., Blakely, R.L., and Zerner, B. (1983) *Methods Enzymol.* **91**, 49-60

73. Kwiatkowski, D.J., Janmey, P.A., Mole, J.E., and Yin, H.L. (1985) *J. Biol. Chem.* **260**, 15232-15238

74. Guilbault, G.G. (1973) " Practical Fluorescence: Theory, Methods, and Techniques", Marcel Dekker Inc., New York

75. Doi, Y., Kim, F., and Kido, S. (1990) *Biochemistry* **29**, 1392-1397

76. Reid, S.W (1990) M.Sc. Thesis, University of British Columbia

77. Ruiz Silva, B.E., Koepf, E.K., Burtnick, L.D., and Turro, N.J., (1992) *Biochem. Cell Biol.* (In Press)

78. Bagshaw, C.R., and Harris, D.A. (1987) "Spectrophotometry & Spectrofluorimetry: A Practical Approach", IRL Press, Oxford

79. Ishikawa, R., Yamashiro, S., and Matsumura, F. (1989) *J. Biol. Chem.*, **264**, 7490-7497

80. Koepf, E.K., and Burtnick, L.D. (1992) *FEBS Lett.*.In Press

81. Doi, Y., Hashimoto, T., Yamaguchi, H., and Vertut-Doi, A. (1991) *Eur. J. Biochem.* **199**, 277-283